NIH Public Access
Author Manuscript
J Immunol. Author manuscript; available in PMC 2009 October 28.

Published in final edited form as:
J Immunol. 2007 April 1; 178(7): 4194–4213.

Cytokine-Mediated Disruption of Lymphocyte Trafficking, Hemopoiesis, and Induction of Lymphopenia, Anemia, and Thrombocytopenia in Anti-CD137-Treated Mice[1]

Liguo Niu[2,*], **Simona Strahotin**[2,*], **Becker Hewes**[2,†], **Benyue Zhang**[*], **Yuanyuan Zhang**[*], **David Archer**[†], **Trent Spencer**[†], **Dirck Dillehay**[§], **Byoung Kwon**[‖], **Lieping Chen**[¶], **Anthony T. Vella**[#], and **Robert S. Mittler**[3,*,‡]

[*]Emory Vaccine Research Center, Emory University School of Medicine, Atlanta, GA 30329

[†]Department of Pediatrics, Emory University School of Medicine, Atlanta, GA 30329

[‡]Department of Surgery, Emory University School of Medicine, Atlanta, GA 30329

[§]Department of Animal Resources, Emory University School of Medicine, Atlanta, GA 30329

[¶]Johns Hopkins University School of Medicine, Department of Dermatology, Baltimore, MD 21205

[‖]The Immunomodulation Research Center, University of Ulsan, Ulsan, Republic of Korea

[#]Department of Immunology, University of Connecticut Health Center, Farmington, CT 06030

Abstract

CD137-mediated signals costimulate T cells and protect them from activation-induced apoptosis; they induce curative antitumor immunity and enhance antiviral immune responses in mice. In contrast, anti-CD137 agonistic mAbs can suppress T-dependent humoral immunity and reverse the course of established autoimmune disease. These results have provided a rationale for assessing the therapeutic potential of CD137 ligands in human clinical trials. In this study, we report that a single 200-μg injection of anti-CD137 given to otherwise naive BALB/c or C57BL/6 mice led to the development of a series of immunological anomalies. These included splenomegaly, lymphadenopathy, hepatomegaly, multifocal hepatitis, anemia, altered trafficking of B cells and CD8 T cells, loss of NK cells, and a 10-fold increase in bone marrow (BM) cells bearing the phenotype of hemopoietic stem cells. These events were dependent on CD8 T cells, TNF-α, IFN-γ, and type I IFNs. BM cells up-regulated Fas, and there was a significant increase in the number of $CD8^+$ T cells that correlated with a loss of $CD19^+$ and Ab-secreting cells in the BM. TCR Vαβ usage was random and polyclonal among liver-infiltrating CD8 T cells, and multifocal $CD8^+$ T cell infiltrates were resolved upon termination of anti-CD137 treatment. Anti-CD137-treated mice developed lymphopenia, thrombocytopenia, and anemia, and had lowered levels of hemoglobin and increased numbers of reticulocytes.

[1]This work was supported by National Institutes of Health Grants R01 CA85860 and R01 AI0592 (to R.S.M.) and RO1-AI52108 (to A.T.V.).

Copyright © 2007 by The American Association of Immunologists, Inc.

3Address correspondence and reprint requests to Dr. Robert S. Mittler, Emory Vaccine Center, 954 Gatewood Road, Atlanta, GA 30329. E-mail address: rmittler@rmy.emory.edu.

[2]L.N., S.S., and B.H. contributed equally to this work.

Disclosures:
The authors have no financial conflict of interest.

NIH-PA Author Manuscript
NIH-PA Author Manuscript
NIH-PA Author Manuscript

NIH-PA Author Manuscript

NIH-PA Author Manuscript

NIH-PA Author Manuscript

Members of the TNFR superfamily play pivotal roles in regulating the survival, proliferation, and differentiation of lymphocytes (1). Anti-CD137/4-1BB/tnfrsf9 mAbs have been shown to induce curative antitumor immunity to established poorly immunogenic tumors in mice (2,3); in some settings, they promote allograft survival (4), reverse established Ab-dependent autoimmune disease (5–8), and enhance antiviral immunity (9–12). These data provide a rationale for the therapeutic evaluation of CD137 ligands in human subjects. However, potential adverse consequences following the administration of these ligands in vivo remain unknown. Expression of CD137 and its natural ligand 4-1BBL is tightly coupled with immune activation, suggesting that promiscuous or constitutive expression of these proteins, or experimental manipulation of their signaling patterns might have deleterious consequences to the host. This latter point was recently illustrated with Abs to another costimulatory molecule. In a human clinical trial, volunteers were injected with superagonist anti-CD28 mAbs (13, 14). Within 2–6 h of administration of a single injection of anti-CD28, all recipients suffered systemic organ failure (15,16). Although agonistic anti-CD137 mAbs do not possess superagonist qualities, they are nevertheless potent inducers of inflammatory cytokine production. Recently, we noted evidence of hepatomegaly in anti-CD137-treated autoimmune New Zealand Black/ White (NZB/W) F_1 mice (our unpublished observation), suggesting that despite the beneficial effects of this treatment on the suppression of autoimmune disease, there was a potential for adverse reactions in treated individuals, and for these reasons we believed it to be prudent to assess the consequences of in vivo use of anti-CD137 mAbs.

CD137 is a costimulatory molecule whose expression was initially thought to be restricted to activated T cells (17). However, later studies revealed that CD137 was expressed on activated NK cells (18); constitutively expressed on a subpopulation of dendritic cells (DC)[4] (19,20); and up-regulated on neutrophils (21), activated monocytes (22), eosinophils (23,24), and mast cells (25). In some cases, it has been reported on the endothelium of blood vessels in metastatic tumors (26). CD137 signaling enhances T cell proliferation and Th1 cytokine production (1) and provides protection to CD8 T cells from activation-induced cell death (27) through NF-κB-mediated activation and up-regulation of the antiapoptotic Bcl-2 family members Bcl-x_L and Bfl-1 (28). In certain settings, anti-CD137 mAbs exacerbate acute graft-vs-host disease and accelerate skin and cardiac allograft rejection (29). Paradoxically, the same reagents enhance the survival of intestinal allografts (4), and when administered during Ag priming, anti-CD137 mAbs effectively suppress T-dependent humoral immunity (30). The latter observation led to the testing of, and the realization that, anti-CD137 mAbs could suppress and reverse the development of autoimmune diseases such as experimental autoimmune encephalomyelitis, systemic lupus erythematosus, and collagen-induced arthritis (5–8). These outcomes have been attributed to enhanced $CD8^+$ T cell survival (27), induction or suppression of CD4 T cell help (30–33), CD8 regulatory T cells (34,35), Th1 cytokine production (29), enhanced $CD8^+$ T cell and NK cell function (18), or regulation of Ag priming by DC (19).

In this study, we report that anti-CD137 mAbs induced multifocal mononuclear cell infiltrates in the livers of BALB/c and C57BL/6 mice. These infiltrates were composed primarily of $CD8^+$ T cells having a diverse TCR Vαβ phenotype. C57BL/6 mice also displayed evidence of dysregulated hemopoiesis in the spleen, lymphocyte trafficking, lymphopenia, thrombocytopenia, and anemia in an anti-CD137 dose-dependent (200–10 μg/mouse) manner. All of these outcomes were T cell and anti-CD137 dependent because they did not occur in SCID, nude, $Rag^{-/-}$, or $CD137^{-/-}$ mice. Anti-CD137-treated, spleen cell-reconstituted, but not B cell-reconstituted $Rag^{-/-}$ mice led to the same outcomes observed in naive BL/6 mice, and identical results were obtained in anti-CD137-injected 4-1BB $ligand^{-/-}$ mice. CD8 T cells, TNF-α, type I IFNs, and IFN-γ were essential for the induction of various aspects of pathology.

[4]Abbreviations used in this paper: DC, dendritic cell; ASC, Ab-secreting cell; BM, bone marrow; CBC, complete blood count; Dbl. Neg., double negative; Dbl. Pos., double positive; LN, lymph node; S1P, sphingosine-1-phosphate; $S1P_1$, S1P receptor 1.

NIH-PA Author Manuscript

NIH-PA Author Manuscript

NIH-PA Author Manuscript

Our findings suggest that anti-CD137-induced activation leads to the production of proinflammatory cytokines, and they in turn induce many, if not all, of the observed anomalies found in anti-CD137-treated mice.

Materials and Methods

Mice and reagents

Female BL/6 mice were purchased from The Jackson Laboratory. CD137-deficient BL/6 mice were generated, as previously described (36). BL/64-1BB ligand-deficient mice were obtained from C. Larsen (Department of Surgery, Emory University, Atlanta, CA) and were initially provided by J. Peschon (Amgen, Seattle, WA). All mice were housed at the Yerkes National Primate Research Center vivarium, where they were maintained according to Institutional Animal Care and Use Committee regulations. The generation of anti-CD137 mAbs has been described (29). Anti-4-1BB ligand mAbs were generated by immunizing Lewis rats with a 4-1BB ligand-human CD8 fusion protein (37), and hybridomas were produced, as previously described (29). Anti-human CD137 mAbs were produced by immunizing Lewis rats with a fusion protein consisting of the extracellular domain of human CD137 with the human IgG1 H chain C domain (37).

Peripheral blood complete blood counts (CBC)

CBC were conducted on peripheral whole blood collected in heparinized Pasteur pipettes by retro-orbital venipuncture. Analysis was conducted using a Sysmex KX-21 automated hematology analyzer (Roche Diagnostics).

Flow cytometry

Fluorochrome-conjugated anti-mouse CD3e (145-2C11), anti-CD4 (GK1.5), anti-CD8 (53–6.7), anti-CD19 (1D3), anti-CD11b (M1/70), anti-CD11c (HL3), anti-CD45 (2D1), CD117 (c-*kit*, 2B8), NK1.1 (PK136), pan NK (DX5), anti-sca-1 (E13-161.7), and anti-CD95 (Fas) (Jo2) were purchased from BD Pharmingen. Cells were preincubated with anti-Fc mAb (2.4G2) and a 10-fold excess of mouse IgG for 10 min before staining. Ab incubations were done on ice for 20 min in PBS with 0.5% BSA and 0.04% NaN_3. Cells were either acquired immediately or fixed with 1% paraformaldehyde and acquired the following day. FACS analysis was conducted using a BD Pharmingen multiparameter LSR-II or BD Pharmingen FACSCalibur flow cytometers. Data analysis was conducted using FlowJo software (Tree Star). Single-cell suspensions of spleen, lymph nodes (LNs), and thymus were prepared by passage through 70-μm cell strainers (BD Pharmingen). Liver and lung were pretreated with digestion buffer (1× HBSS, 20 mM HEPES (pH 7.4), 0.0175% collagenase IV, 5 mM $CaCl_2$, 0.0005% DNase I, and 0.0025% hyaluronidase) for 90 min at room temperature. Dead cells, debris, and liver and lung cells were then removed by Ficoll-Hypaque discontinuous density-gradient centrifugation. Bone marrow (BM) was obtained by irrigating femurs and tibias with cold PBS using a 25-gauge needle. RBC were lysed with ammonium chloride RBC lysis buffer containing the following: 8.29 g/L NH_4Cl, 1.00 g/L $KHCO_3$, and 0.037 g/L EDTA (pH 7.27).

Anti-CD137 treatment of mice

Eight- to 12-wk-old BL/6 female mice, CD137-deficient, or 4-1BB ligand-deficient mice were injected i.p. with 200 μg of rat anti-CD137 (3H3), rat anti-human CD137 (26G6), or rat IgG (Sigma-Aldrich) once weekly, as indicated. All Abs were standardized to a concentration of 1 mg/ml, and endotoxin levels were nil.

NIH-PA Author Manuscript

NIH-PA Author Manuscript

NIH-PA Author Manuscript

ELISA and ELISPOT

NUNC maxisorp 96-well plates were coated with Sigma-Aldrich rat IgG (I-4131) at 20 μg/ml at 4°C overnight. They were then washed with PBS with 0.05% Tween 20. They were blocked with 2% BSA in PBS overnight at 4°C. After washing, serum samples were serially diluted with PBS containing 1% BSA and 0.05% Tween 20 and incubated for 3 h at room temperature. Anti-rat IgG (H+L) was used as a standard (Biomedia). After extensive washing, goat anti-mouse IgG (H+L) HRP (Invitrogen Life Technologies) was added and incubated at room temperature for 2 h. Plates were then washed and developed with urea-buffered PBS containing hydrogen peroxide and *o*-phenylenediamine. The reaction was stopped with 50 μl of H_2SO_4 per well. Plates were read at 490 mm with a Spectra Max 340 (Molecular Devices). For ELISPOT assays, Millipore MAHA N4510 plates (Millipore) were coated with goat anti-mouse IgG, IgM, and IgA (Invitrogen Life Technologies) at 100 μl/well, 5 μg/ml overnight at 4°C. They were blocked with RPMI1640 complete medium for 2 h. Splenocytes were plated at 10^6 in 100 μl of RPMI 1640 complete medium, serially diluted 3-fold, and incubated for 5 h at 37°C. Biotinylated goat anti-mouse IgG (Invitrogen Life Technologies) was added, and plates were incubated overnight at 4°C. Plates were developed with HRP-conjugated avidin-D (Vector Laboratories) at 5 μg/ml for 1 h and 3-amino-9-ethylcarbazole substrate. Spots were read using ImmunoSpot ELISPOT reader and software (Cellular Technology).

Histology

Organs were fixed in 10% formalin overnight and paraffin embedded. Slices (5 μm) were H&E stained. Photomicrographs were taken with a Zeiss Axioskop 2 microscope.

CBCs

Mice were anesthetized with isoproterenol and bled retro-orbitally through heparinized capillary tubes into microtainers containing EDTA (BD Pharmingen). A total of 50 μl of blood was analyzed with a blood cell analyzer (Kx-21; Sysmex).

Statistical analysis

Statistical significance at the 95% confidence interval was conducted using unpaired, two-sided Student's *t* test, or one-way ANOVA, depending on the nature of the study groups.

CFSE labeling and BrdU incorporation

Lymphocytes were resuspended at 2×10^7/ml in PBS containing 2.5 mM CFSE (Molecular Probes) and incubated at 37°C with periodic shaking for 5 min. The suspension was washed twice with 15 ml of cold PBS and resuspended in Dulbecco's PBS at 2×10^7/ml for tail vein injection. For BrdU labeling, mice were injected i.p. with 200 μl of a 10 mg/ml solution of BrdU in sterile Dulbecco's PBS. Four hours later, the mice were euthanized and single-cell suspensions of lymphocytes were intracellular stained with FITC anti-BrdU following the manufacturer's recommendations (BD Immunocytometry Systems).

Results

Gross pathology and histopathology

The fact that anti-CD137-injected NZB/W F_1 autoimmune mice developed hepatomegaly was of immediate concern. However, this outcome may have been related to their predisposition to develop autoimmune disease. Therefore, we injected naive BALB/c mice once weekly over a 5-wk period with 200 μg of anti-CD137 or rat IgG mAbs. We initially used BALB/c mice because they shared the H-2^d haplotype with NZB/W F_1 (H-$2^{d/z}$) mice, and later switched to C57BL/6 mice to take advantage of CD137-deficient and 4-1BB ligand-deficient mice that were on the BL/6 background. Because both strains of mice developed indistinguishable

NIH-PA Author Manuscript

NIH-PA Author Manuscript

NIH-PA Author Manuscript

pathology, this report focuses solely on data obtained from anti-CD137- or rat IgG-injected BL/6 mice. Mice were euthanized 1 wk following the indicated number of weekly 200-μg i.p. Ab injections. Spleens, livers, and left and right inguinal LNs obtained from anti-CD137-injected mice were markedly enlarged, and this correlated with elapsed time of treatment (Fig. 1*a*). Rat IgG-injected mice exhibited minor enlargement of the spleen and LNs, but this was generally small (<10%). In contrast to splenomegaly and lymphadenopathy that continued to increase over the treatment period, hepatomegaly plateaued within 2 wk of treatment (Fig. 1*a*). Mice given a single 200-μg dose of anti-CD137 and assayed 5 wk later also developed splenomegaly, hepatomegaly, and lymphadenopathy (Fig. 1*b*). However, in this instance, the level of splenomegaly and hepatomegaly was less severe than that seen following multiple injections of anti-CD137. Similarly, five weekly 10 μg doses of the 3H3 anti-CD137 mAb, or any of several independently generated anti-CD137 mAbs of varying isotype and fine specificity were sufficient to cause the same effects (Fig. 1*c*). In contrast, a single 10- or 30-μg injection of anti-CD137 was without effect (data not shown). These data indicate that the specificity or isotype of the 3H3 mAb used in these studies was not the cause of these events. All Abs were endotoxin free, as judged by standard *Limulus* agglutination assays. The 3H3 is a rat IgG2a isotype Ab having a serum $t_{1/2}$ in mice of 7 days. Histology was performed on all tissues from anti-CD137- or rat IgG-injected mice 1 wk following the fifth weekly 200-μg injection. In all instances, spleen, liver, and lungs from rat IgG-injected mice appeared normal (Fig. 1*d*, *left panels*), whereas the LNs, liver, and lungs of anti-CD137-injected mice displayed mononuclear cell infiltrates (Fig. 1*d*, *middle* and *right panels*), and in the case of the spleen dissolution of the typical histological architecture and marked evidence of extramedullary hemopoiesis (Fig. 1*d*, *middle* and *right panels*). Livers from rat IgG-treated mice were normal (Fig. 1*d*, *left panel*), whereas livers from anti-CD137-treated mice revealed evidence of multifocal hepatitis (Fig. 1*d*, *middle panel*) with prominent perivascular accumulation of mononuclear cells and the presence of apoptotic hepatocytes around the vasculature (Fig. 1*d*, *middle right panel*). Indicative of possible liver inflammation, we observed a 2-fold elevation in serum glutamic oxaloacetic transaminase and serum glutamic pyruvate transaminase levels in the serum of the mice within 2 wk of treatment (Fig. 1*e*). Although the increase in transaminase levels can be caused by other factors, and was only 2-fold over controls, the observation was highly reproducible and no other signs of pathology could explain this occurrence. Furthermore, FACS analysis revealed that >30% of liver-infiltrating $CD4^+$ T cells and ~15% of infiltrating $CD8^+$ T cells expressed Fas ligand, suggesting that these T cells could induce apoptosis of hepatocytes that express Fas (CD95) on their surface. Although the lungs of anti-CD137-treated mice were normal on gross inspection, they contained a 10-fold increase in the number of infiltrating peribronchiolar mononuclear cells (Fig. 1*d*, *middle panel*), and these cells were observed migrating into the bronchiolar space (Fig. 1*d*, *right panel*).

In the spleen, we found a direct correlation between spleen weight and cell number during the first 21 days of treatment (Fig. 1*a* and Fig. 2*a*). However, by day 28 we observed a decreasing trend in spleen cell numbers (Fig. 2*a*). However, this decrease did not reach statistical significance until after week 4 for $CD8^+$ T cells (Fig. 2*a*). In contrast, we observed a more rapid loss of $CD19^+$ B cells and $CD4^+$ T cells by weeks 2 and 3, respectively (Fig. 2*a*). This was not due to CD19 down-regulation because there was a concomitant loss of B220 and surface Ig^+ B cells (data not shown). Thus, splenic B cells were either being deleted or trafficking elsewhere. This is in contrast to what we observed in collagen-induced arthritis-susceptible DBA/1J mice, in which spleen cell numbers actually increased at ~30 days of anti-CD137 treatment (6). The reason for this discrepancy is not immediately evident and may simply reflect, for reasons unknown, a difference in the kinetics of lymphocyte trafficking in the two strains of mice. It should also be pointed out that DBA/1J mice had far fewer spleen cells at basal levels than did BALB/c or C57BL/6 mice. In addition to the loss of splenic B cells, we observed a near complete loss of NK and NKT cells in the spleens of anti-CD137-injected mice (Fig. 2*b*). Phenotypic analysis of splenic T cells for CD44 and CD62L expression

NIH-PA Author Manuscript

NIH-PA Author Manuscript

NIH-PA Author Manuscript

revealed a small increase in the frequency of $CD44^{high}CD62L^{low/-}$ memory T cells in anti-CD137-treated mice; however, the majority of cells expressed high levels of CD62L (Fig. 2*b*). Furthermore, we observed an increase in the frequency of T cells that had down-regulated their expression of CD45RB and did not express the early activation marker CD69 (Fig. 2*b*). Phenotypic analysis of LN cells to a large degree mirrored what was seen in the spleen. In this instance too, there was an absence of NK and NKT cells. With regard to their activation state, LN T cells significantly down-regulated CD45RB expression with no change in memory phenotype (Fig. 2*c*). One means by which lymphocytes are retained within LNs is by up-regulating expression of CD69. Studies by Shiow et al. (38) have shown that the activation Ag CD69 complexes with sphingosine-1-phosphate (S1P) receptor 1 ($S1P_1$) and has an antagonistic effect on $S1P_1$-mediated egress of lymphocytes from the LNs and thymus. However, we did not find evidence of CD69 expression on LN lymphocytes from anti-CD137-treated mice.

Within the livers of rat IgG-injected mice, we found very high frequencies of NKT cells (>30%) and relatively high frequencies of NK cells (Fig. 2*d*). In contrast, we found a 2-fold reduction in the frequency of liver NKT cells, but little change in the frequency of NK cells in the livers of anti-CD137-injected mice, although the intensity of NK1.1 expression on these cells had decreased substantially (Fig. 2*d*). However, when we determined the absolute numbers of liver NKT and NK cells in rat IgG- and anti-CD137-treated mice, there was no difference in NKT cell number between the two groups of treated mice, whereas there were increased numbers of NK cells in anti-CD137-injected mice that almost reached statistical significance (Fig. 2*d*). NK cells in mice and in humans display different phenotypic markers, such as CD16 and CD56 in humans. In mice this is true for the IL-7Rα (CD127) expression and the requirement for GATA-3, depending upon whether they are BM or thymus derived. Vosshenrich et al. (39) have found that splenic NK cells do not express GATA-3, whereas BM and liver NK cells express low levels of GATA-3, but thymic NK cells express high levels of GATA-3. Both BM- and thymus-derived NK cells can be found in the LNs of normal mice. Because we do not find any NK cells in the LNs of anti-CD137-treated mice, we can conclude that both BM- and thymus-derived NK cells are equally affected by anti-CD137 mAb treatment. Thus, it is interesting to note that anti-CD137 treatment fails to eliminate NK cells from the liver; instead, it modestly increased their numbers. In the lungs, the frequency (Fig. 2*e*) and absolute number of NK cells (data not shown) increase dramatically in anti-CD137-treated mice. Thus, it is possible that the absence of NK cells from the spleen and LNs is a reflection of their trafficking to the liver and lungs. One possibility is that NK cell loss or trafficking is coupled to CD137 expression on these cells, and it can be argued that expression either prevents their loss/trafficking or enhances it. The generation of CD137-deficient BM chimeras will help to address this question. Among liver-infiltrating T cells there was a loss of CD44 and, to a lesser extent, CD62L expression (Fig. 2*d*). Surprisingly, there were fewer $CD45RB^{low}$ and $CD69^+$ T cells in the livers of anti-CD137-treated mice compared with rat IgG-treated animals (Fig. 2*d*).

We next analyzed various T cell subsets in each tissue for expression of the above markers. We found that $CD8^+$ T cells and TCR $\alpha\beta^+$ $CD3^+CD4^-CD8^-$ (double-negative (Dbl. Neg.)) T cells in the spleen displayed the most significant reduction in CD45RB expression (Fig. 3*a*), indicating they had previously encountered an activation signal, and, in keeping with this view, this population had the most significant increase in CD44 expression. CD62L expression, although down-regulated on both $CD4^+$ and $CD8^+$ T cells, was highly up-regulated on the Dbl. Neg. subset, providing evidence that these cells had recently been activated. CD69 expression increased modestly on all three subsets (Fig. 3*a*). The precise role of Dbl. Neg. T cell activation in anti-CD137-treated mice remains to be determined. Previous studies have shown that Dbl. Neg. T cells can function as natural suppressor cells (40,41), generate MHC class I-restricted CTL responses (42), and undergo expansion during CMV infection in mice, in which they may play a protective role against infection (43). In contrast, their presence and expansion correlate

NIH-PA Author Manuscript

NIH-PA Author Manuscript

NIH-PA Author Manuscript

with systemic lupus erythematosus disease progression in MRL$^{lpr-/-}$ mice (44). Interestingly, and contrary to our observations in this work, anti-CD137 treatment of MRL$^{lpr-/-}$ mice leads to a reduction in number of these cells (7). In the LNs, CD45RB was down-regulated on CD4$^+$ T cells and Dbl. Neg. cells, whereas increased CD44 expression was most evident on CD8$^+$ T cells; no changes were observed in CD62L and CD69 expression on LN cells (Fig. 3*a*).

Among liver T cell populations, in addition to the subsets of T cells described above, we found a significant number of CD3$^+$CD4$^+$CD8$^+$ (double-positive (Dbl. Pos.)) T cells. T cells from rat IgG-injected mice, with the exception of CD4$^+$ T cells, consisted of CD45RB^{high} cells (Fig. 3*b*). In contrast, in anti-CD137-injected mice, CD45RB expression was highly down-regulated on liver CD8$^+$ T cells and Dbl. Neg. T cells (Fig. 3*b*), whereas CD62L down-regulation was most evident on Dbl. Neg. and Dbl. Pos. T cells in these mice (Fig. 3*b*). Analysis of lung-derived T cells revealed that anti-CD137 treatment blocked CD45RB down-regulation on CD4$^+$ and CD8$^+$ T cells, and to some extent, on Dbl. Pos. T cells. In contrast, we observed a mixed phenotype within the Dbl. Neg. T cell subset, in which both reduced and increased CD45RB expression was found on populations of these cells (Fig. 3*c*). CD44 expression was down-regulated on the Dbl. Neg. T cell population of anti-CD137-treated mice, up-regulated on the Dbl. Pos. T cell population, highly up-regulated on CD8$^+$ T cells, and modestly up-regulated on CD4$^+$ T cells (Fig. 3*c*). CD62L expression, in contrast, was up-regulated on CD8$^+$ T cells and Dbl. Pos. T cells in the lungs of anti-CD137-injected mice, whereas CD69 expression was either unchanged or modestly down-regulated on these T cell subsets (Fig. 3*c*).

We observed three striking features in the BM of anti-CD137-treated mice. The first was the marked loss of CD19$^+$ cells (Fig. 4*a*); the second was a 6- to 10-fold increase in the number of infiltrating CD8$^+$ T cells (Fig. 4*b*); and the third, and perhaps most striking, was a > 10-fold increase in CD45$^+$ KSL, i.e., Sca-1$^+$ c-*kit*$^+$ *lin*$^-$ hemopoietic stem cells (Fig. 4*c*). It has been shown that the regulation of hemopoiesis and cellular proliferation in the BM is in part controlled by TNF-α, in which TNF-α potently suppressed the development of primitive and committed BM progenitors in both mice and humans (45,46). It has also been shown that Fas-mediated apoptosis regulates BM progenitor cell development (47), and that TNF-α and IFN-γ induce Fas expression on T cells (48). We, therefore, examined the role of CD8 T cells, Fas (CD95) expression, and TNF-α on the loss of CD19$^+$ BM cells from rat IgG- or anti-CD137-injected mice 1 wk following the last of five weekly injections of Ab. We first assessed the role of CD8 T cells in the loss of CD19$^+$ BM progenitor cells by injecting CD8 T cell-deficient mice with rat IgG or anti-CD137. However, these studies ruled out CD8$^+$ T cells as mediators of CD19$^+$ BM cell loss because we found the same degree of CD19$^+$ BM cell depletion in CD8 T cell-deficient mice as in wild-type mice (data not shown). We next determined whether TNF-α was responsible for the loss of B cell progenitors. BL/6 mice were injected with anti-CD137 or rat IgG once weekly with or without 200 μg of a neutralizing anti-TNF-α mAb for 5 wk, and 1 wk later the mice were euthanized and their BM collected and FACS analyzed. In addition, TNF-α-deficient mice were also treated with anti-CD137 or rat IgG. In both sets of experiments, we found the same degree of CD19$^+$ BM cell and Ab-secreting cell (ASC) loss as that seen in wild-type mice (data not shown). We next examined, and found, marked up-regulation of Fas expression on BM cells, and this correlated with the concomitant loss of CD19$^+$ BM cells (Fig. 4*d*), suggesting that the loss of these cells and perhaps other progenitor cells may occur in part through Fas-mediated signaling. However, when we treated MRL$^{lpr-/-}$ mice with anti-CD137, we still found the same level of CD19$^+$ BM cell loss (data not shown). Previous studies have reported the suppression of B cell development in a BM transplantation model in which the donor BM differed from the recipient at several minor MHC loci. Suppression of B cell development was caused by donor T cell-mediated graft-vs-host disease reactions and was dependent upon the production of IFN-γ by these alloreactive T cells

NIH-PA Author Manuscript

NIH-PA Author Manuscript

NIH-PA Author Manuscript

(49). Because anti-CD137 stimulation induces the production of high levels of IFN-γ, we tested whether this cytokine played a role in the loss of $CD19^+$ cells by using IFN-γ-deficient mice or BL/6 mice injected weekly with neutralizing anti-IFN-γ mAbs. In contrast to all other strains tested, BM $CD19^+$ progenitors in anti-CD137-injected, IFN-γ-deficient mice were the same in number as those found in rat IgG-injected IFN-γ-deficient mice, or wild-type mice (Fig. 4*e*). To determine whether BM ASC were affected by anti-CD137 treatment, mice were injected with PBS, rat IgG, or anti-CD137, as described above. BM was collected and assayed by overnight culture on ELISPOT plates coated with sheep anti-mouse IgG. Whereas PBS-injected mice had on average 280 ASC/10^6 BM cells, anti-CD137-injected mice had <40 ASC/10^6 BM cells (Fig. 4*f*). These data are in keeping with our previous studies showing that anti-CD137 mAbs suppress the induction of T-dependent humoral immunity in mice (5,6,30), and important to this study, to itself.

LN $CD8^+$ T and B cell proliferation

In contrast to splenic lymphocytes, $CD4^+$ and $CD8^+$ T cells and $CD19^+$ B cells in the inguinal LNs significantly increased in number following anti-CD137 treatment (Fig. 2*a*). To assess whether this was due to lymphocyte trafficking, proliferation, or both, we injected 1–2 × 10^6 CFSE-labeled BL/6 CD45.1 congenic splenocytes i.v. into naive BL/6 CD45.2 mice before beginning anti-CD137 treatment 10 days later. Twenty-one days after the last of three weekly injections of anti-CD137, the mice were euthanized and inguinal LNs were removed. LN $CD45.1^+$ CFSE-labeled T and B cells were counted and proliferation was measured by FACS. Over 50% of $CD8^+$ T cells from anti-CD137-treated mice (black histogram) had undergone multiple rounds of cell division compared with 17% for rat IgG (red histogram)-treated mice (Fig. 5*a*, *left panel*). Thus, we could not determine whether CD8 T cells in anti-CD137-injected mice were proliferating within, or trafficked to the LNs following proliferation, and this was true for CD4 T cells (data not shown). However, this was not the case for B cells, in which <30% (mean of 27 ± 4% $n = 4$) of $CD45.1^+CD3^-$ $B220^+$ B cells (black histogram) had undergone cell division, a frequency that was comparable with that observed in rat IgG (red histogram)-injected mice (Fig. 5*a*, *right panel*). Still, there was a 3- to 7-fold increase in the total number of LN B cells in anti-CD137-treated mice (Fig. 2*a*), suggesting that B cells had emigrated to the inguinal LNs. To further address this issue, and to determine the level of in situ proliferation at various time points following anti-CD137 treatment, we i.p. injected anti-CD137-treated and rat IgG-treated mice with BrdU 1 day following the second weekly injection of Ab. Four hours later, the mice were euthanized and inguinal LNs were collected (as were other tissues), and single-cell suspensions were stained with fluorochrome-conjugated mAbs specific for CD3, CD4, CD8, and CD19. The cells were permeabilized and stained with a fluorochrome-conjugated anti-BrdU mAb (BD Immunocytometry Systems) and analyzed by FACS. However, although high levels of proliferation were seen in the BM and thymus, there was no difference between the two groups of treated mice, and there was little evidence of lymphocyte proliferation in any of the other tissues studied (data not shown). Therefore, a second experiment was performed in which the mice were given two weekly injections of Ab. One day following the third weekly injection, the mice were injected with BrdU, and 4 h later euthanized. Inguinal LN cells (Fig. 5*b*) as well as spleen, liver, and lung were analyzed, as described above (Fig. 6*c*). Analysis of LN B and T cells from rat IgG- or anti-CD137-injected mice showed similar levels of BrdU incorporation, suggesting that the major cause of the increase in absolute numbers of these cells in the LNs of anti-CD137-treated mice was caused by cell trafficking and not proliferation.

Splenic T cells and lung- and liver-infiltrating T cells

Lung and liver mononuclear cells from mice that received two to three injections of 200 μg of anti-CD137 mAbs or rat IgG were stained with fluorescence-conjugated mAbs, and the frequency of cell lineages was determined by FACS analysis. The number of non-T cells in

NIH-PA Author Manuscript

NIH-PA Author Manuscript

NIH-PA Author Manuscript

lungs and livers from anti-CD137-treated mice was equal to controls (data not shown). In the lungs, there was no change in the frequency (data not shown) or absolute numbers of $CD4^+$ T cells (Fig. 6*a*), whereas $CD8^+$ T cell number increased almost 10-fold (Fig. 6*a*). In the liver, there was a dramatic increase in both $CD4^+$ and $CD8^+$ T cells (Fig. 6*a*). Proliferation of spleen-, liver-, and lung-infiltrating CD8 T cells was determined by CFSE dilution, as described above, in mice given 1 × 3 weekly 200-μg anti-CD137 or rat IgG injections. Whereas a significant number of CD8 T cells in the spleen and virtually all CD8 T cells in the livers of anti-CD137-injected mice were proliferating, CD8 T cells in the lungs from anti-CD137- or rat IgG-injected mice had undergone a couple of cell divisions either before or following their entry into the lungs (Fig. 6*b*). Regardless, there was no notable change between treated and control groups. $CD8^+$ T cell proliferation was then determined by BrdU incorporation, as described above, 24 h following the last of three weekly injections of either anti-CD137 or rat IgG. Again, although massive proliferation was observed in the BM of both groups of mice, and was in fact increased in anti-CD137-injected mice and in the thymus, in which no differences in proliferation between the groups were seen, we observed only a slight difference in BrdU incorporation by liver $CD8^+$ T cells obtained from anti-CD137-treated mice (Fig. 6*c*).

Lymphocyte proliferation

Lymphocyte proliferation was studied in greater detail to determine whether the observed changes in cell number in various tissues were a result of proliferation or trafficking. In addition to B cells and single-positive T cells, we examined $CD3^+CD4^-CD8^-$ and $CD3^-CD19^-$ subsets. In the thymus, we did not observe any changes in the frequency or absolute number of proliferating mature T cells, B cells, or among thymocyte subpopulations in mice injected with anti-CD137 or rat IgG (data not shown). In the BM, we observed a slight, but reproducible increase in the proliferation of $CD3^-CD19^-$ cells in anti-CD137-injected vs rat IgG-injected mice (46.2 vs 34.7%). In the spleens, we observed a slight decrease in proliferation within the $CD3^+CD4^-CD8^-$ population and a 3-fold increase in $CD3^-CD19^-$ lymphocytes (Fig. 7*a*), whereas in the LNs we observed an increase in the proliferative rate of $CD3^+$ Dbl. Neg. lymphocytes (Fig. 7*b*). In the livers, we did not observe any significant change in the proliferation of any subset examined (Fig. 7*c*), whereas we found a 2-fold increase in the frequency of $CD4^+$ T cell proliferation in the lungs and a 14% increase in proliferation of $CD3^+$ Dbl. Neg. lymphocytes (Fig. 7*d*). From these data we can conclude that the major changes in lymphocyte numbers in the LNs, livers, and lungs, and CD8 T cell accumulation in the BM of anti-CD137-injected mice are largely the result of altered lymphocyte trafficking.

TCR specificity and pathophysiology

T cells are essential for the manifestation of the pathologies found in anti-CD137-treated mice because no changes were seen in anti-CD137-treated $Rag^{-/-}$, B cell-reconstituted $Rag^{-/-}$, SCID, or nude mice (data not shown). However, when anti-CD137 was given to T and B cell-reconstituted $Rag^{-/-}$ mice, the mice developed all of the pathologies observed in BL/6 mice. TCR specificity and the state of T cell activation in anti-CD137-treated mice were studied by injecting naive lymphocytic choriomeningitis virus $gp_{33–41}$-specific BL/6 P14 TCR $Rag^{-/-}$ transgenic, and BL/6 OT-II OVA-specific TCR transgenic $Rag^{-/-}$ mice weekly, over a 5-wk period, with anti-CD137 mAbs. In neither case did we observe any effect of anti-CD137, including activation markers or CFSE dilution (data not shown), suggesting that naive T cells are not targets of anti-CD137 mAbs. To determine whether Ag-activated P14 $CD8^+$ T cells could generate the observed pathologies, we activated P14 cells in vitro for 5 days with $gp_{33–41}$ peptide-pulsed DC in the presence of IL-2 and transferred them along with syngeneic B cells into recipient $Rag^{-/-}$ recipients, and the mice were injected weekly with anti-CD137 over a 4-wk period. The T cells continued to proliferate in anti-CD137-treated mice and increased in number at a rate faster than that seen in homeostatic proliferation (data not shown). Nevertheless, the mice developed none of the pathologies seen in anti-CD137-treated normal

NIH-PA Author Manuscript

NIH-PA Author Manuscript

NIH-PA Author Manuscript

naive mice (data not shown), suggesting that activated P14 CD8 T cells alone were insufficient to induce pathology, or that TCR specificity was an important component to the establishment of pathology. To address potential autoreactivity and TCR clonality of CD8 T cells in the livers of anti-CD137-injected mice, we injected naive mice with anti-CD137 or rat IgG once weekly for 5 wk. Livers were removed 1 wk after the final Ab injection and mononuclear cells were isolated. Because CD8 T cell-deficient mice do not develop hepatitis and CD4 T cell-deficient mice do (see below), we only examined the frequency and number of $CD8^+$ T cells bearing different Vα and Vβ specificities. Data from three experiments showed increased frequencies of T cells bearing diverse TCR *Vαβ* gene products, indicating a lack of clonality and, by extension, a low probability that the expansion of CD8 T cells represented an autoimmune reaction (Fig. 8). Indeed, mice given anti-CD137 for 26 wk never developed signs of autoimmune disease; once anti-CD137 injections were terminated, the livers of these returned to normal, suggesting that hepatitis may be caused primarily by proinflammatory cytokines.

Peripheral mononuclear cells and blood elements

Anti-CD137-treated mice developed evidence of extramedullary hemopoiesis in the spleen. To determine whether the hemopoietic system in these mice was under stress, we studied the effect of anti-CD137 treatment on PBMC number. Mice were injected weekly with 200 μg of anti-CD137 or rat IgG and bled every 10–14 days over a 4-mo time span. White blood cell counts dropped precipitously within 2 wk of treatment (Fig. 9*a*) due to the onset of lymphopenia (Fig. 9*b*), whereas the number of monocytes increased 2- to 3-fold (Fig. 9*c*). By the fifth week, anti-CD137-treated mice developed marked thrombocytopenia (Fig. 9*d*). Platelet consumption can occur in response to high systemic levels of TNF-α (50,51), and we have found that anti-CD137 induces TNF-α production (our unpublished observations). The onset of thrombocytopenia in anti-CD137-injected mice is noteworthy because platelets are a major source of S1P (52–54). High S1P levels in the blood relative to the tissues are essential for the formation of a concentration gradient needed for the egress of $S1P_1$-expressing lymphocytes from the thymus and LNs (55). As shown above, we find a significant number of nonproliferating B cells as well as T cells in the LNs of anti-CD137-injected mice, suggesting that the loss of platelets in these mice may be responsible for lowering serum S1P levels. As an indirect indicator that this may be the case, we find that $S1P_1$ mRNA is up-regulated on lymphocytes in anti-CD137-injected mice by a factor of 2 compared with rat IgG-treated controls (data not shown). This being the case, one would expect that these cells would rapidly egress from this tissue, but they do not. Other changes in the CBC of anti-CD137-injected mice included an increase in the number of reticulocytes (Fig. 9*e*), an observation that correlated with a 25% decrease in hemoglobin levels (Fig. 9*f*) and a low hematocrit (data not shown). Spleens from anti-CD137-injected mice, rather than having a deep dark red color, were pink and pale in color (data not shown). Reduced CBC could be accelerated in anti-CD137-treated, but not rat IgG-injected mice by bleeding them every other day (100 μl) for 1 wk. This stress led to a severely diminished hematocrit and death of 90% of the mice ($n = 10$) within 1 wk.

CD8 and CD4 T cell-mediated pathology

We determined whether $CD8^+$ and/or $CD4^+$ T cells were required for the onset of pathology. CD8 T $cell^{-/-}$ and CD4 T $cell^{-/-}$ mice received 200 μg of anti-CD137 mAbs or rat IgG once weekly for 5 wk and were euthanized 1 wk later, and lymphoid tissues and selected organs were removed and analyzed. CD8 T $cell^{-/-}$ mice developed splenomegaly and lymphadenopathy (Fig. 10*a*), suggesting that CD4 T cells and/or NK cells could induce these reactions. Whereas NK cells may play a role in the induction of hepatomegaly, it is unlikely they induce splenomegaly or lymphadenopathy, because virtually all NK cells are depleted from the spleens and LNs of anti-CD137-injected mice. However, $CD8^{-/-}$ mice did not develop hepatomegaly (Fig. 10*a*) or multifocal hepatitis (data not shown). CD8 T $cell^{-/-}$ mice nevertheless had reduced numbers of $CD19^+$ BM cells (Fig. 10*a*), and like BL/6 mice, CD8 T

NIH-PA Author Manuscript

NIH-PA Author Manuscript

NIH-PA Author Manuscript

cell$^{-/-}$ mice had elevated BM KSL cells (Fig. 10*a*) and fewer splenic CD19^{+} B cells (Fig. 10*a*) with B cell accumulation in the LNs as observed in wild-type mice (data not shown). In contrast, anti-CD137 mAb-treated CD4 T cell$^{-/-}$ mice developed pathology identical to that seen in BL/6 mice (Fig. 10*b*).

Cytokine-deficient mice

We have found that TNF-α serum levels are elevated and prolonged following anti-CD137 treatment of lymphocytic choriomeningitis virus-infected mice (C. H. Maris, B. Zhang, I. Foell, J. Whitmire, L. Niu, J. Song, J. Tan, E. Sotomayor, B. S. Kwon, A. T. Vella, J. Jacob, R. Ahmed, and R. S. Mittler, manuscript in preparation). Therefore, we assessed the contribution of TNF-α in promoting anti-CD137-induced pathologies. Anti-CD137-treated BL/6 TNF-α$^{-/-}$ mice did not develop splenomegaly, lymphadenopathy, or hepatomegaly (Fig. 11, *a–c*, respectively). Furthermore, the mice did not develop lymphopenia (data not shown). This is in keeping with previous reports showing that mediators of innate immunity, including type I IFNs and TNF-α, can shut down systemic shutdown of egress of lymphocytes from secondary lymphoid tissues, and as a result, a loss of these cells in the circulation (56–58). Whereas the livers of anti-CD137-injected mice had a 4-fold increase in numbers of CD8 T cells (Fig. 11*d*), they did not show any signs of liver pathology or elevated levels of transaminases (data not shown). Consistent with data from CD8$^{-/-}$ mice, the absence of TNF-α did not alter the loss of CD19^{+} B cells from the spleen (Fig. 11*e*), nor the increase in the number of B cells and CD8 T cells in the LNs (Fig. 11, *f* and *g*, respectively). The observations observed in TNF-α-deficient mice were also observed by injecting neutralizing anti-TNF-α mAbs into anti-CD137-treated BL/6 mice (data not shown).

Because we had shown previously that anti-CD137 enhances production of proinflammatory cytokines such as IFN-γ by CD8^{+} T cells (29), we assessed the effects of anti-CD137 mAb injection of BL/6 IFN-γ$^{-/-}$ mice. Although IFN-γ$^{-/-}$ mice developed splenomegaly, hepatomegaly, multifocal hepatitis (data not shown), lymphadenopathy (Fig. 12*a*), and an increase in the numbers of BM KSL cells (data not shown), we found no change in the number of LN CD19^{+} B and CD8^{+} T cells (Fig. 12*a*). These outcomes were also observed in anti-CD137-injected BL/6 mice coinjected with neutralizing anti-IFN-γ mAbs (data not shown).

Plasmacytoid DC are efficient producers of type I IFNs (59). We, and others, have shown that DC can express CD137 (19,20). Among DC subpopulations, we found that plasmacytoid express the highest density of CD137 receptors on their surface, and as a population, they contain the highest frequency of CD137-positive DC (our unpublished observation). We considered that cross-linking CD137 on pDC might contribute to the anti-CD137-induced phenotype through up-regulation of type I IFN production. Be- cause type I IFNs bind a common receptor (59), we used type I IFNR$^{-/-}$ mice to assess whether these cytokines were required for anti-CD137-induced pathology. The mice were injected once weekly for 3 wk with 200 μg of anti-CD137 or rat IgG. One week after the last injection, the mice were euthanized, and organs and cells were analyzed. All of the anti-CD137-treated mice developed splenomegaly, lymphadenopathy, hepatomegaly, and multifocal hepatitis (data not shown). However, unlike that seen in other mice, the frequency and absolute number of CD19^{+} BM cells were normal (Fig. 12*b*). Most striking, these mice had normal frequen- cies and absolute numbers of KSL^{+} BM cells (Fig. 12*b*), and nor- mal numbers of CD19^{+} B cells and CD8 T cells in the LNs (Fig. 12*b*). Furthermore, the number of splenic CD19^{+} B cells was greatly increased (Fig. 12*b*).

Discussion

Based on encouraging preclinical data from mouse studies, antihuman CD137 mAbs are entering clinical trials for treating cancer, rheumatoid arthritis, and systemic lupus

NIH-PA Author Manuscript

NIH-PA Author Manuscript

NIH-PA Author Manuscript

erythematosus. However, little is known regarding potential adverse events associated with repeated in vivo administration of anti-CD137. Having knowledge of such reactions, should they occur, would be of considerable value in guiding the design of clinical trials, especially because earlier studies of several receptor-ligand pairs of the TNFR-TNF superfamilies such as TRAIL-DR5 (60,61), Fas ligand-Fas (62,63), and CD70-CD27 (64) have been found to induce severe toxicity when given in vivo, or during chronic stimulation.

The results of our study demonstrate that although the CD137 signaling pathway is another example in which its therapeutic manipulation holds promise for its clinical applicability, such manipulation can lead to unexpected adverse events, potential pathology, and the alteration of normal immune system or organ function. One injection of anti-CD137 mAb at 10 or 0.5 mg/kg given once weekly over a 5-wk period induced a series of adverse events in normal mice that appear to be confined to the immune and hemopoietic systems. These occurrences may ultimately adversely affect the normal function of several major organs, including the liver, lungs, spleen, and BM. CD137 receptor cross-linking, $CD8^+$ T cells, and the production of TNF-α, IFN-γ, and IFN-α were found to be essential for the induction of these adverse events. It is unclear whether T cells are the direct targets of anti-CD137 mAbs, or whether they are indirectly affected by cytokines, or chemokines produced by other lineages of CD137-expressing cells. Studies addressing this question are now in progress. Liver-infiltrating $CD8^+$ T cells and TNF-α were essential for the induction of hepatitis, and the absence of either prevented disease in anti-CD137-injected mice. As best we could discern, these liver $CD8^+$ T cells were not Vαβ clonally restricted or oligoclonal in nature. Rather, Vαβ usage varied from experiment to experiment, and in some instances, the TCR Vαβ representation of expanded CD8 T cells in the liver mirrored that observed in IgG-injected mice, leading us to believe that activated $CD8^+$ TNF-α-secreting T cells trafficking to the liver are not likely responding to liver-associated Ags. These observations also argue against autoimmune involvement, and favor cytokine-induced inflammation as the primary cause of liver pathology. Further evidence against autoimmune involvement comes from the observation that anti-CD137-injected mice recover normal liver function following cessation of treatment. Studies in IFN-γ, TNF-α, and type I IFNR-deficient mice led us to conclude that TNF-α and CD8 T cells are critical to the induction of splenomegaly, lymphadenopathy, hepatomegaly, and multifocal hepatitis, because none of these adverse events developed in their absence. In contrast, IFN-γ and type I IFNs appeared to be essential for T and B cell trafficking, and for the 10-fold increase in the number of BM hemopoietic cells, because these events were not observed in type I $IFNR^{-/-}$ mice and IFN-$\gamma^{-/-}$ mice, and were markedly reduced in anti-CD137-treated wild-type mice injected with neutralizing IFN-γ mAbs. This observation is consistent with previous studies showing that TNF-α and type I and II IFNs induce severe liver toxicity, thrombocytopenia, and disruption of hemopoiesis (65–70). Mechanisms regulating the marked increase in the number of BM KSL cells following anti-CD137 remain unclear. Accelerated or enhanced production of these cells within the BM is unlikely because hemopoietic cells express receptors for type I IFNs (71), and type I IFNs suppress proliferation of these cells via G_1 arrest mediated by Cip/Kip and Ink4 cyclin-dependent kinase inhibitors (72). Therefore, we favor the view that type I IFNs allow for KSL cell accumulation while blocking their proliferation through G_1 arrest.

Questions regarding the adverse effects of anti-CD137 on immune and hemopoietic cell function remain. Chief among them with respect to their clinical potential is whether a therapeutically effective dose can be established that does not cause, or at least minimizes, these adverse reactions, and whether the same or other adverse events will be observed in nonhuman primates and human subjects. It will be important to understand the extent of anti-CD137-mediated suppression of normal BM development, the fate and differentiation potential of expanded BM hemopoietic stem cells, and the regulation of extramedullary hemopoiesis in the spleen. We have yet to identify changes in the production of chemokines and expression

NIH-PA Author Manuscript

NIH-PA Author Manuscript

NIH-PA Author Manuscript

of their receptors that are important for lymphocyte trafficking to and from the LNs and spleen and into tissues of the body. Studies are now underway to examine the effects of anti-CD137 treatment on the histology and immunohistology of LNs and Peyer's patches obtained from mice given repeated injections of this Ab. Likewise, we are measuring the levels of serum S1P and the regulation of $S1P_1$ expression on lymphocytes in anti-CD137-injected mice. Previous studies showed a loss of B cells in mice overexpressing 4-1BB ligand under regulation of the MHC class II promoter and enhancer (73), and in anti-CD137-treated *BL/6*$^{lpr-/-}$ mice (7), respectively. In the latter study, anti-CD137-mediated B cell depletion appeared to be independent of Fas- and TNFR-mediated signaling, but dependent on IFN-γ, in which it correlated with an increase in the number of GR-1^+ immature macrophages. In our studies, we did not observe any increase in the population size of these macrophages, and we also observed a significant loss in splenic B cells in anti-CD137-treated IFN-$\gamma^{-/-}$ mice. Perhaps the difference between the two studies is that in our model B cells are not being deleted, but instead undergo massive migration from the spleen to other lymphoid tissues. Finally, we are in the process of testing humanized anti-CD137 in nonhuman primates, in which they are cross-reactive and T cell activating, to see whether they induce similar responses to those observed in mice.

Acknowledgments

We thank Rossana Chung and Emily Burnham for their excellent technical contributions, and Dr. Tania Watts for her critical review of this manuscript.

References

1. Watts TH. TNF/TNFR family members in costimulation of T cell responses. Annu. Rev. Immunol 2005;23:23–68. [PubMed: 15771565]
2. Melero I, Shuford WW, Newby SA, Aruffo A, Ledbetter JA, Hellstrom KE, Mittler RS, Chen L. Monoclonal antibodies against the 4-1BB T-cell activation molecule eradicate established tumors. Nat. Med 1997;3:682–685. [PubMed: 9176498]
3. Melero I, Bach N, Hellstrom KE, Aruffo A, Mittler RS, Chen L. Amplification of tumor immunity by gene transfer of the co-stimulatory 4-1BB ligand: synergy with the CD28 costimulatory pathway. Eur. J. Immunol 1998;28:1116–1121. [PubMed: 9541607]
4. Wang J, Guo Z, Dong Y, Kim O, Hart J, Adams A, Larsen CP, Mittler RS, Newell KA. Role of 4-1BB in allograft rejection mediated by $CD8^+$ T cells. Am. J. Transplant 2003;3:543–551. [PubMed: 12752310]
5. Foell J, Strahotin S, O'Neil SP, McCausland MM, Suwyn C, Haber M, Chander PN, Bapat AS, Yan XJ, Chiorazzi N, et al. CD137 costimulatory T cell receptor engagement reverses acute disease in lupus-prone NZB × NZW F_1 mice. J. Clin. Invest 2003;111:1505–1518. [PubMed: 12750400]
6. Foell JL, Diez-Mendiondo BI, Diez OH, Holzer U, Ruck P, Bapat AS, Hoffmann MK, Mittler RS, Dannecker GE. Engagement of the CD137 (4-1BB) costimulatory molecule inhibits and reverses the autoimmune process in collagen-induced arthritis and establishes lasting disease resistance. Immunology 2004;113:89–98. [PubMed: 15312139]
7. Sun Y, Chen HM, Subudhi SK, Chen J, Koka R, Chen L, Fu YX. Costimulatory molecule-targeted antibody therapy of a spontaneous autoimmune disease. Nat. Med 2002;8:1405–1413. [PubMed: 12426559]
8. Seo SK, Choi JH, Kim YH, Kang WJ, Park HY, Suh JH, Choi BK, Vinay DS, Kwon BS. 4-1BB-mediated immunotherapy of rheumatoid arthritis. Nat. Med 2004;10:1088–1094. [PubMed: 15448685]
9. Halstead ES, Mueller YM, Altman JD, Katsikis PD. In vivo stimulation of CD137 broadens primary antiviral $CD8^+$ T cell responses. Nat. Immunol 2002;3:536–541. [PubMed: 12021777]
10. Tan JT, Whitmire JK, Murali-Krishna K, Ahmed R, Altman JD, Mittler RS, Sette A, Pearson T, Larsen CP. 4-1BB costimulation is required for protective anti-viral immunity after peptide vaccination. J. Immunol 2000;164:2320–2325. [PubMed: 10679066]

NIH-PA Author Manuscript NIH-PA Author Manuscript NIH-PA Author Manuscript

11. Bukczynski J, Wen T, Ellefsen K, Gauldie J, Watts TH. Costimulatory ligand 4-1BBL (CD137L) as an efficient adjuvant for human antiviral cytotoxic T cell responses. Proc. Natl. Acad. Sci. USA 2004;101:1291–1296. [PubMed: 14745033]
12. Bukczynski J, Wen T, Wang C, Christie N, Routy JP, Boulassel MR, Kovacs CM, Macdonald KS, Ostrowski M, Sekaly RP, et al. Enhancement of HIV-specific CD8 T cell responses by dual costimulation with CD80 and CD137L. J. Immunol 2005;175:6378–6389. [PubMed: 16272290]
13. Tacke M, Hanke G, Hanke T, Hunig T. CD28-mediated induction of proliferation in resting T cells in vitro and in vivo without engagement of the T cell receptor: evidence for functionally distinct forms of CD28. Eur. J. Immunol 1997;27:239–247. [PubMed: 9022025]
14. Luhder F, Huang Y, Dennehy KM, Guntermann C, Muller I, Winkler E, Kerkau T, Ikemizu S, Davis SJ, Hanke T, Hunig T. Topological requirements and signaling properties of T cell-activating, anti-CD28 antibody superagonists. J. Exp. Med 2003;197:955–966. [PubMed: 12707299]
15. Wadman M. London's disastrous drug trial has serious side effects for research. Nature 2006;440:388–389. [PubMed: 16554763]
16. Marshall E. Drug trials: violent reaction to monoclonal antibody therapy remains a mystery. Science 2006;311:1688–1689. [PubMed: 16556805]
17. Pollok KE, Kim YJ, Zhou Z, Hurtado J, Kim KK, Pickard RT, Kwon BS. Inducible T cell antigen 4-1BB: analysis of expression and function. J. Immunol 1993;150:771–781. [PubMed: 7678621]
18. Melero I, Johnston JV, Shufford WW, Mittler RS, Chen L. NK1.1 cells express 4-1BB (CDw137) costimulatory molecule and are required for tumor immunity elicited by anti-4-1BB monoclonal antibodies. Cell. Immunol 1998;190:167–172. [PubMed: 9878117]
19. Wilcox RA, Chapoval AI, Gorski KS, Otsuji M, Shin T, Flies DB, Tamada K, Mittler RS, Tsuchiya H, Pardoll DM, Chen L. Cutting edge: expression of functional CD137 receptor by dendritic cells. J. Immunol 2002;168:4262–4267. [PubMed: 11970964]
20. Futagawa T, Akiba H, Kodama T, Takeda K, Hosoda Y, Yagita H, Okumura K. Expression and function of 4-1BB and 4-1BB ligand on murine dendritic cells. Int. Immunol 2002;14:275–286. [PubMed: 11867564]
21. Heinisch IV, Daigle I, Knopfli B, Simon HU. CD137 activation abrogates granulocyte-macrophage colony-stimulating factor-mediated antiapoptosis in neutrophils. Eur. J. Immunol 2000;30:3441–3446. [PubMed: 11093162]
22. Schwarz H, Valbracht J, Tuckwell J, von Kempis J, Lotz M. ILA, the human 4-1BB homologue, is inducible in lymphoid and other cell lineages. Blood 1995;85:1043–1052. [PubMed: 7849293]
23. Heinisch IV, Bizer C, Volgger W, Simon HU. Functional CD137 receptors are expressed by eosinophils from patients with IgE-mediated allergic responses but not by eosinophils from patients with non-IgE-mediated eosinophilic disorders. J. Allergy Clin. Immunol 2001;108:21–28. [PubMed: 11447378]
24. Reali C, Curto M, Sogos V, Scintu F, Pauly S, Schwarz H, Gremo F. Expression of CD137 and its ligand in human neurons, astrocytes, and microglia: modulation by FGF-2. J. Neurosci. Res 2003;74:67–73. [PubMed: 13130507]
25. Nishimoto H, Lee SW, Hong H, Potter KG, Maeda-Yamamoto M, Kinoshita T, Kawakami Y, Mittler RS, Kwon BS, Ware CF, et al. Costimulation of mast cells by 4-1BB, a member of the tumor necrosis factor receptor superfamily, with the high-affinity IgE receptor. Blood 2005;106:4241–4248. [PubMed: 16123219]
26. Broll K, Richter G, Pauly S, Hofstaedter F, Schwarz H. CD137 expression in tumor vessel walls: high correlation with malignant tumors. Am. J. Clin. Pathol 2001;115:543–549. [PubMed: 11293902]
27. Takahashi C, Mittler RS, Vella AT. Cutting edge: 4-1BB is abona fide CD8 T cell survival signal. J. Immunol 1999;162:5037–5040. [PubMed: 10227968]
28. Lee HW, Park SJ, Choi BK, Kim HH, Nam KO, Kwon BS. 4-1BB promotes the survival of $CD8^+$ T lymphocytes by increasing expression of Bcl-x_L and Bfl-1. J. Immunol 2002;169:4882–4888. [PubMed: 12391199]
29. Shuford WW, Klussman K, Tritchler DD, Loo DT, Chalupny J, Siadak AW, Brown TJ, Emswiler J, Raecho H, Larsen CP, et al. 4-1BB costimulatory signals preferentially induce $CD8^+$ T cell proliferation and lead to the amplification in vivo of cytotoxic T cell responses. J. Exp. Med 1997;186:47–55. [PubMed: 9206996]

NIH-PA Author Manuscript

NIH-PA Author Manuscript

NIH-PA Author Manuscript

30. Mittler RS, Bailey TS, Klussman K, Trailsmith MD, Hoffmann MK. Anti-4-1BB monoclonal antibodies abrogate T cell-dependent humoral immune responses in vivo through the induction of helper T cell anergy. J. Exp. Med 1999;190:1535–1540. [PubMed: 10562327]
31. Zheng G, Wang B, Chen A. The 4-1BB costimulation augments the proliferation of $CD4^+CD25^+$ regulatory T cells. J. Immunol 2004;173:2428–2434. [PubMed: 15294956]
32. Choi BK, Bae JS, Choi EM, Kang WJ, Sakaguchi S, Vinay DS, Kwon BS. 4-1BB-dependent inhibition of immunosuppression by activated $CD4^+CD25^+$ T cells. J. Leukocyte Biol 2004;75:785–791. [PubMed: 14694186]
33. Wilcox RA, Tamada K, Flies DB, Zhu G, Chapoval AI, Blazar BR, Kast WM, Chen L. Ligation of CD137 receptor prevents and reverses established anergy of $CD8^+$ cytolytic T lymphocytes in vivo. Blood 2004;103:177–184. [PubMed: 12969968]
34. Myers L, Takahashi C, Mittler RS, Rossi RJ, Vella AT. Effector CD8 T cells possess suppressor function after 4-1BB and Toll-like receptor triggering. Proc. Natl. Acad. Sci. USA 2003;100:5348–5353. [PubMed: 12695569]
35. Myers L, Croft M, Kwon BS, Mittler RS, Vella AT. Peptide-specific CD8 T regulatory cells use IFN-γ to elaborate TGF-β-based suppression. J. Immunol 2005;174:7625–7632. [PubMed: 15944263]
36. Kwon BS, Hurtado JC, Lee ZH, Kwack KB, Seo SK, Choi BK, Koller BH, Wolisi G, Broxmeyer HE, Vinay DS. Immune responses in 4-1BB (CD137)-deficient mice. J. Immunol 2002;168:5483–5490. [PubMed: 12023342]
37. Loo DT, Chalupny NJ, Bajorath J, Shuford WW, Mittler RS, Aruffo A. Analysis of 4-1BBL and laminin binding to murine 4-1BB, a member of the tumor necrosis factor receptor superfamily, and comparison with human 4-1BB. J. Biol. Chem 1997;272:6448–6456. [PubMed: 9045669]
38. Shiow LR, Rosen DB, Brdickova N, Xu Y, An J, Lanier LL, Cyster JG, Matloubian M. CD69 acts downstream of interferon-αβ to inhibit S1P1 and lymphocyte egress from lymphoid organs. Nature 2006;440:540–544. [PubMed: 16525420]
39. Vosshenrich CA, Garcia-Ojeda ME, Samson-Villeger SI, Pasqualetto V, Enault L, Goff OR, Corcuff E, Guy-Grand D, Rocha B, Cumano A, et al. A thymic pathway of mouse natural killer cell development characterized by expression of GATA-3 and CD127. Nat. Immunol 2006;7:1217–1224. [PubMed: 17013389]
40. Strober S, Dejbachsh-Jones S, Van Vlasselaer P, Duwe G, Salimi S, Allison JP. Cloned natural suppressor cell lines express the $CD3^+CD4^-$ $CD8^-$ surface phenotype and the α, β heterodimer of the T cell antigen receptor. J. Immunol 1989;143:1118–1122. [PubMed: 2526181]
41. Young KJ, DuTemple B, Phillips MJ, Zhang L. Inhibition of graft-versus-host disease by double-negative regulatory T cells. J. Immunol 2003;171:134–141. [PubMed: 12816991]
42. Mieno M, Suto R, Obata Y, Udono H, Takahashi T, Shiku H, Nakayama E. $CD4^-CD8^-$ T cell receptor αβ T cells: generation of an in vitro major histocompatibility complex class I specific cytotoxic T lymphocyte response and allogeneic tumor rejection. J. Exp. Med 1991;174:193–201. [PubMed: 1905338]
43. Hossain MS, Takimoto H, Ninomiya T, Yoshida H, Kishihara K, Matsuzaki G, Kimura G, Nomoto K. Characterization of $CD4^-CD8^-$ $CD3^+$ T-cell receptor-$\alpha\beta^+$ T cells in murine cytomegalovirus infection. Immunology 2000;101:19–29. [PubMed: 11012749]
44. Gutierrez-Ramos JC, Andreu JL, Revilla Y, Vinuela E, Martinez C. Recovery from autoimmunity of MRL/*lpr* mice after infection with an interleukin-2/vaccinia recombinant virus. Nature 1990;346:271–274. [PubMed: 1973822]
45. Rogers JA, Berman JW. TNF-α inhibits the further development of committed progenitors while stimulating multipotential progenitors in mouse long-term bone marrow cultures. J. Immunol 1994;153:4694–4703. [PubMed: 7963539]
46. Jacobsen SE, Jacobsen FW, Fahlman C, Rusten LS. TNF-α, the great imitator: role of p55 and p75 TNF receptors in hematopoiesis. Stem Cells 1994;12:111–126. [PubMed: 7535144]
47. Maciejewski J, Selleri C, Anderson S, Young NS. Fas antigen expression on $CD34^+$ human marrow cells is induced by interferon γ and tumor necrosis factor α and potentiates cytokine-mediated hematopoietic suppression in vitro. Blood 1995;85:3183–3190. [PubMed: 7538820]

NIH-PA Author Manuscript

NIH-PA Author Manuscript

NIH-PA Author Manuscript

48. Oyaizu N, McCloskey TW, Than S, Hu R, Kalyanaraman VS, Pahwa S. Cross-linking of CD4 molecules up-regulates Fas antigen expression in lymphocytes by inducing interferon-γ and tumor necrosis factor-α secretion. Blood 1994;84:2622–2631. [PubMed: 7522637]
49. Garvy BA, Elia JM, Hamilton BL, Riley RL. Suppression of B-cell development as a result of selective expansion of donor T cells during the minor H antigen graft-versus-host reaction. Blood 1993;82:2758–2766. [PubMed: 8219228]
50. Tacchini-Cottier F, Vesin C, Redard M, Buurman W, Piguet PF. Role of TNFR1 and TNFR2 in TNF-induced platelet consumption in mice. J. Immunol 1998;160:6182–6186. [PubMed: 9637537]
51. Senaldi G, Piguet PF. Mortality and platelet depletion occur independently of fibrinogen consumption in murine models of tumor necrosis factor-mediated systemic inflammatory responses. Cytokine 1998;10:382–389. [PubMed: 9619377]
52. Yatomi Y, Ruan F, Hakomori S, Igarashi Y. Sphingosine-1-phosphate: a platelet-activating sphingolipid released from agonist stimulated human platelets. Blood 1995;86:193–202. [PubMed: 7795224]
53. Yatomi Y, Igarashi Y, Yang L, Hisano N, Qi R, Asazuma N, Satoh K, Ozaki Y, Kume S. Sphingosine 1-phosphate, a bioactive sphingolipid abundantly stored in platelets, is a normal constituent of human plasma and serum. J. Biochem 1997;121:969–973. [PubMed: 9192741]
54. Igarashi Y, Yatomi Y. Sphingosine 1-phosphate is a blood constituent released from activated platelets, possibly playing a variety of physiological and pathophysiological roles. Acta Biochim. Pol 1998;45:299–309. [PubMed: 9821862]
55. Matloubian M, Lo CG, Cinamon G, Lesneski MJ, Xu Y, Brinkmann V, Allende ML, Proia RL, Cyster JG. Lymphocyte egress from thymus and peripheral lymphoid organs is dependent on S1P receptor 1. Nature 2004;427:355–360. [PubMed: 14737169]
56. Degre M. Influence of polyinosinic:polycytidylic acid on the circulating white blood cells in mice. Proc. Soc. Exp. Biol. Med 1973;142:1087–1091. [PubMed: 4694806]
57. Korngold R, Blank KJ, Murasko DM. Effect of interferon on thoracic duct lymphocyte output: induction with either poly I:poly C or vaccinia virus. J. Immunol 1983;130:2236–2240. [PubMed: 6187846]
58. Young AJ, Seabrook TJ, Marston WL, Dudler L, Hay JB. A role for lymphatic endothelium in the sequestration of recirculating γδ T cells in TNF-α-stimulated lymph nodes. Eur. J. Immunol 2000;30:327–334. [PubMed: 10602056]
59. Theofilopoulos AN, Baccala R, Beutler B, Kono DH. Type I interferons (αβ) in immunity and autoimmunity. Annu. Rev. Immunol 2005;23:307–336. [PubMed: 15771573]
60. Jo M, Kim TH, Seol DW, Esplen JE, Dorko K, Billiar TR, Strom SC. Apoptosis induced in normal human hepatocytes by tumor necrosis factor-related apoptosis-inducing ligand. Nat. Med 2000;6:564–567. [PubMed: 10802713]
61. Zheng SJ, Wang P, Tsabary G, Chen YH. Critical roles of TRAIL in hepatic cell death and hepatic inflammation. J. Clin. Invest 2004;113:58–64. [PubMed: 14702109]
62. Lacronique V, Mignon A, Fabre M, Viollet B, Rouquet N, Molina T, Porteu A, Henrion A, Bouscary D, Varlet P, et al. Bcl-2 protects from lethal hepatic apoptosis induced by an anti-Fas antibody in mice. Nat. Med 1996;2:80–86. [PubMed: 8564847]
63. Redondo C, Flores I, Gonzalez A, Nagata S, Carrera AC, Merida I, Martinez AC. Linomide prevents the lethal effect of anti-Fas antibody and reduces Fas-mediated ceramide production in mouse hepatocytes. J. Clin. Invest 1996;98:1245–1252. [PubMed: 8787688]
64. Tesselaar K, Arens R, van Schijndel GM, Baars PA, van der Valk MA, Borst J, van Oers MH, van Lier RA. Lethal T cell immunodeficiency induced by chronic costimulation via CD27-CD70 interactions. Nat. Immunol 2003;4:49–54. [PubMed: 12469117]
65. Spriggs DR, Sherman ML, Frei E III, Kufe DW. Clinical studies with tumor necrosis factor. Ciba Found. Symp 1987;131:206–227. [PubMed: 3330011]
66. Lehmann V, Freudenberg MA, Galanos C. Lethal toxicity of lipopolysaccharide and tumor necrosis factor in normal and d-galactosamine-treated mice. J. Exp. Med 1987;165:657–663. [PubMed: 3819645]

NIH-PA Author Manuscript

NIH-PA Author Manuscript

NIH-PA Author Manuscript

67. Leist M, Gantner F, Jilg S, Wendel A. Activation of the 55 kDa TNF receptor is necessary and sufficient for TNF-induced liver failure, hepatocyte apoptosis, and nitrite release. J. Immunol 1995;154:1307–1316. [PubMed: 7822799]

68. Aman MJ, Keller U, Derigs G, Mohamadzadeh M, Huber C, Peschel C. Regulation of cytokine expression by interferon-α in human bone marrow stromal cells: inhibition of hematopoietic growth factors and induction of interleukin-1 receptor antagonist. Blood 1994;84:4142–4150. [PubMed: 7994029]

69. Lin Q, Dong C, Cooper MD. Impairment of T and B cell development by treatment with a type I interferon. J. Exp. Med 1998;187:79–87. [PubMed: 9419213]

70. Deonarain R, Verma A, Porter AC, Gewert DR, Platanias LC, Fish EN. Critical roles for IFN-β in lymphoid development, myelopoiesis, and tumor development: links to tumor necrosis factor α. Proc. Natl. Acad. Sci. USA 2003;100:13453–13458. [PubMed: 14597717]

71. Giron-Michel J, Weill D, Bailly G, Legras S, Nardeux PC, Azzarone B, Tovey MG, Eid P. Direct signal transduction via functional interferon-αβ receptors in $CD34^+$ hematopoietic stem cells. Leukemia 2002;16:1135–1142. [PubMed: 12040445]

72. Sangfelt O, Erickson S, Einhorn S, Grander D. Induction of Cip/Kip and Ink4 cyclin dependent kinase inhibitors by interferon-α in hematopoietic cell lines. Oncogene 1997;14:415–423. [PubMed: 9053838]

73. Zhu G, Flies DB, Tamada K, Sun Y, Rodriguez M, Fu YX, Chen L. Progressive depletion of peripheral B lymphocytes in 4-1BB (CD137) ligand/I-Eα-transgenic mice. J. Immunol 2001;167:2671–2676. [PubMed: 11509610]

NIH-PA Author Manuscript
NIH-PA Author Manuscript
NIH-PA Author Manuscript

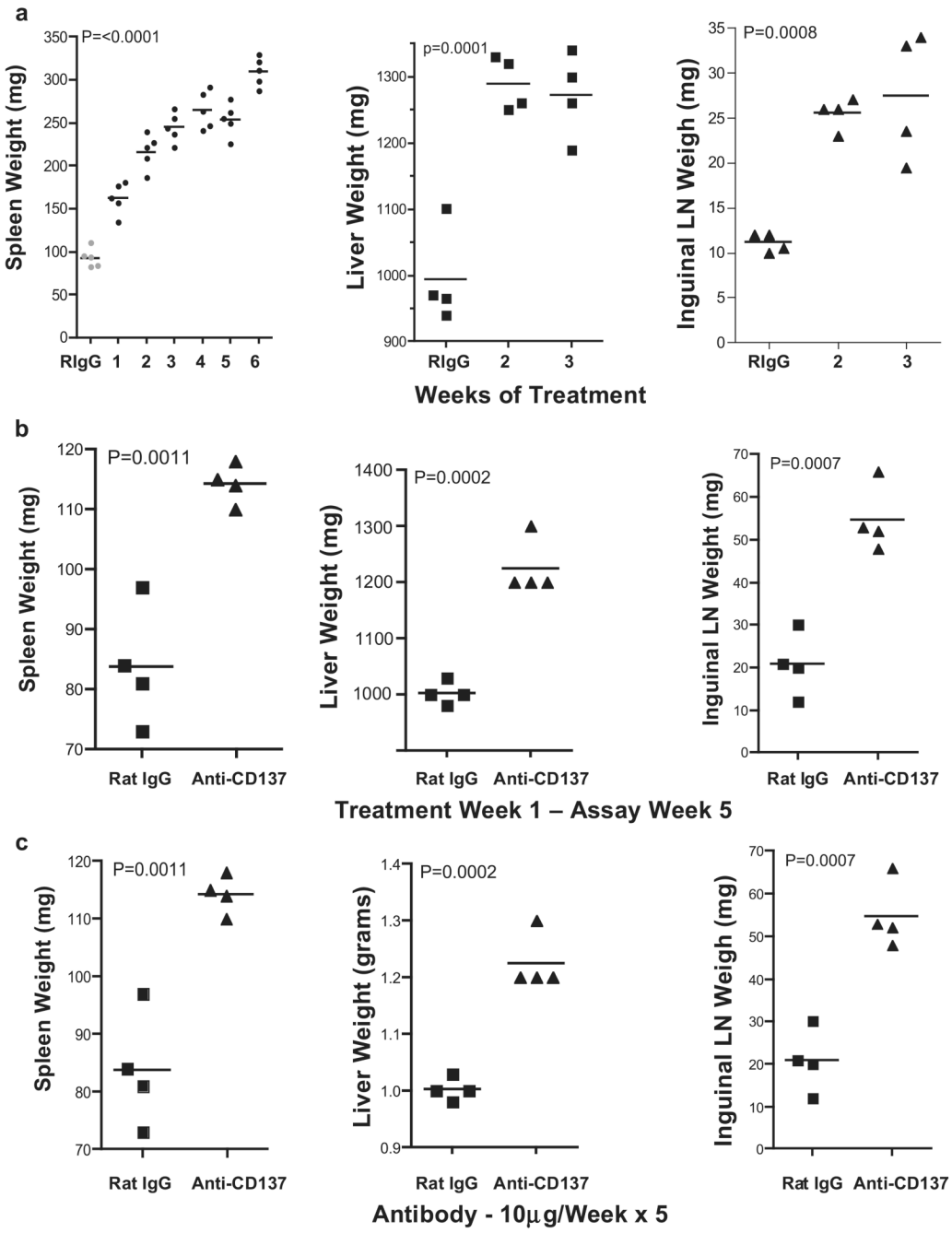

NIH-PA Author Manuscript

NIH-PA Author Manuscript

NIH-PA Author Manuscript

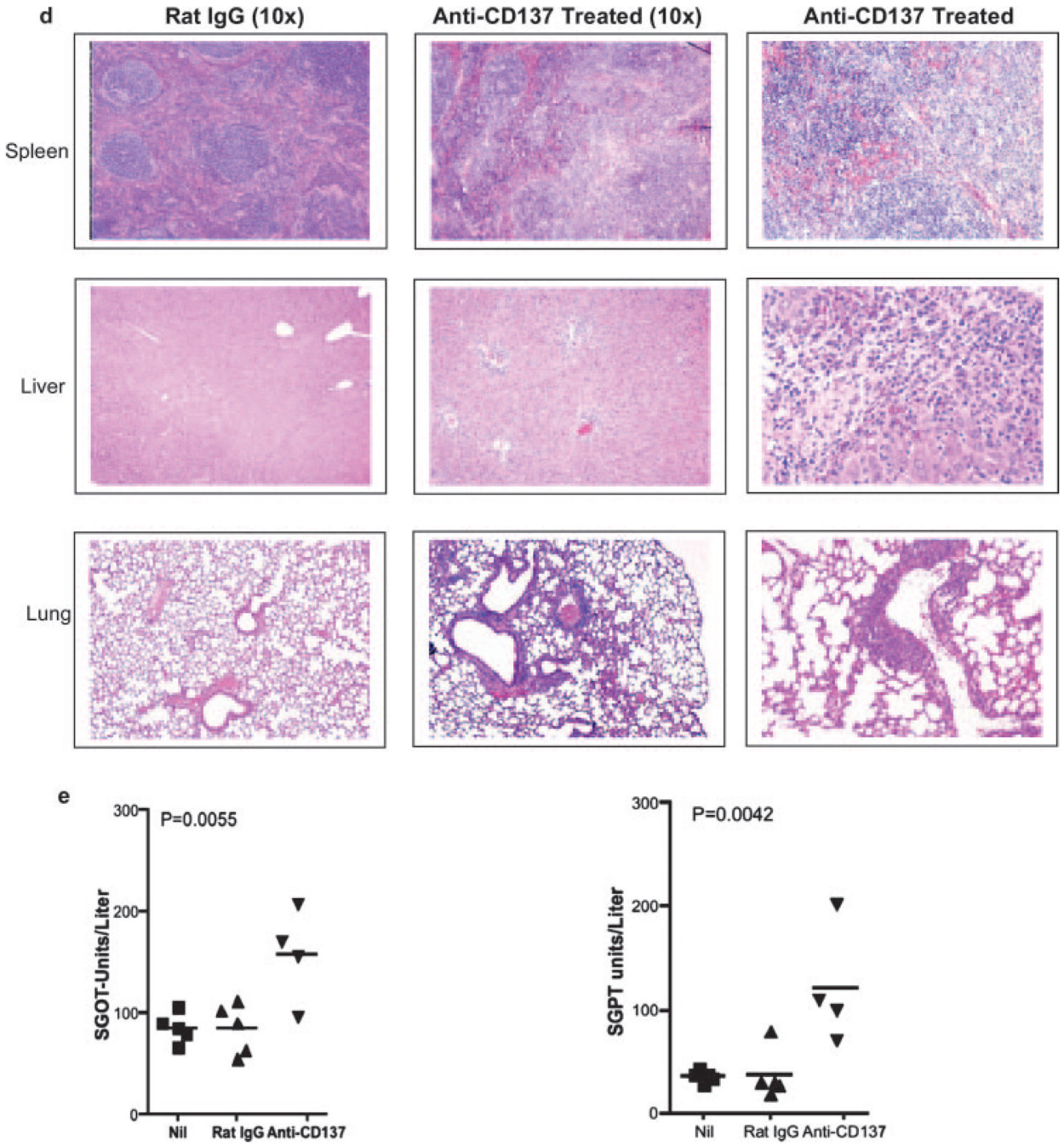

FIGURE 1.

Pathology and transaminase levels. *a*, BL/6 female mice were injected i.p. weekly with 200 μg of anti-CD137 or rat IgG, as indicated. One week after the indicated number of injections, the mice were euthanized, and spleens, livers, and inguinal nodes (combined) were weighed. A single 3-wk time point is shown for rat IgG-injected mice. *b*, Organ weight 5 wk after a single 200-μg i.p. injection of rat IgG or anti-CD137 mAbs. The data shown are representative of one of three separate experiments. *c*, Organ weight 5 wk after five weekly 10-μg i.p. injections of rat IgG or anti-CD137 mAbs. *d*, Spleens, livers, and lungs were obtained from mice 1 wk following the fifth weekly i.p. injection of 200 μg of rat IgG or anti-CD137. Tissues were fixed, paraffin embedded, cut into 5-μm sections, H&E stained, and photographed. *e*,

NIH-PA Author Manuscript

NIH-PA Author Manuscript

NIH-PA Author Manuscript

Before euthanization, the mice were bled, and serum was collected and analyzed for levels of glutamic oxaloacetic transaminase and glutamic pyruvate transaminase. One of two experiments is shown, and symbols represent individual mice.

NIH-PA Author Manuscript
NIH-PA Author Manuscript
NIH-PA Author Manuscript

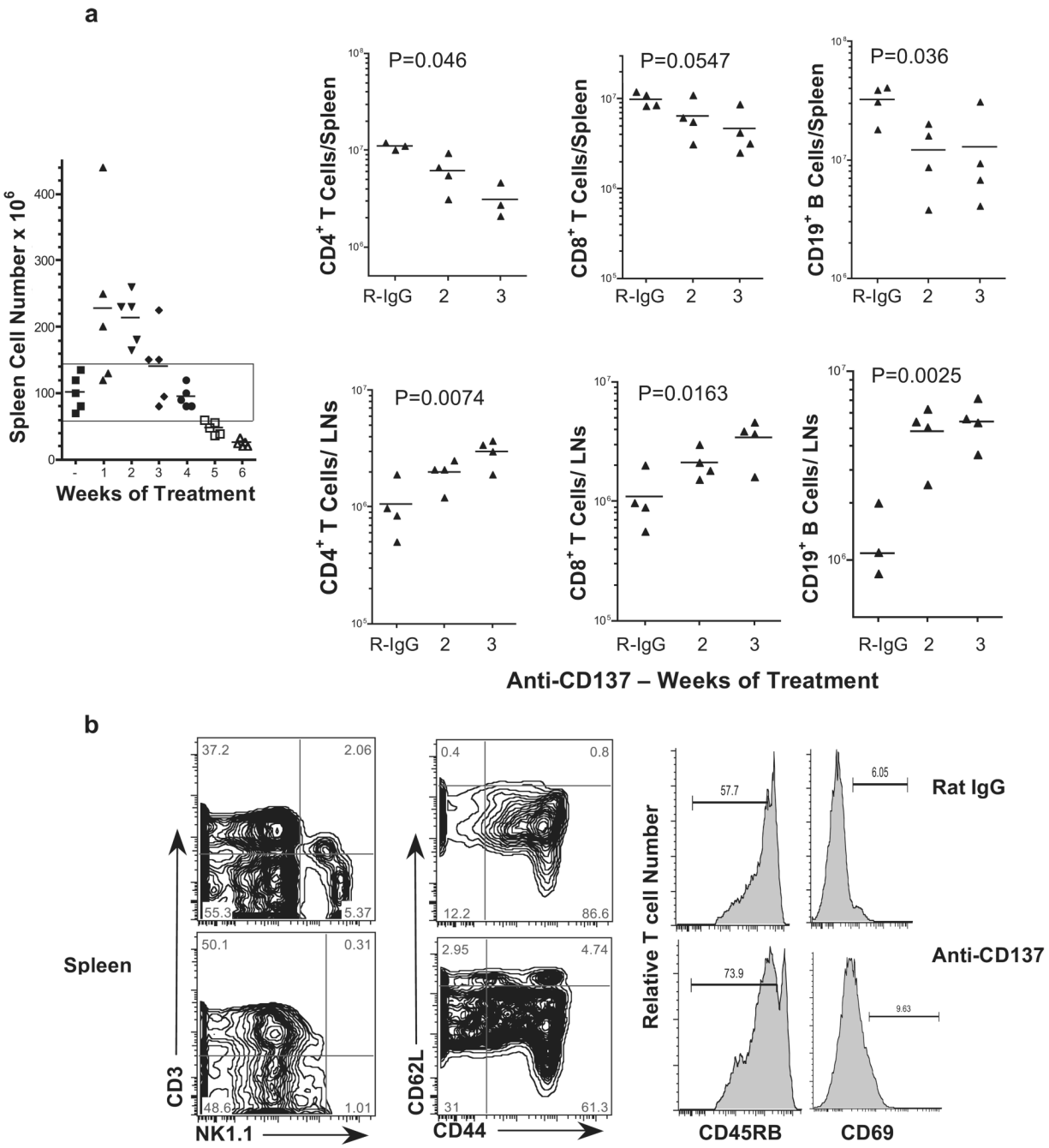

NIH-PA Author Manuscript
NIH-PA Author Manuscript
NIH-PA Author Manuscript

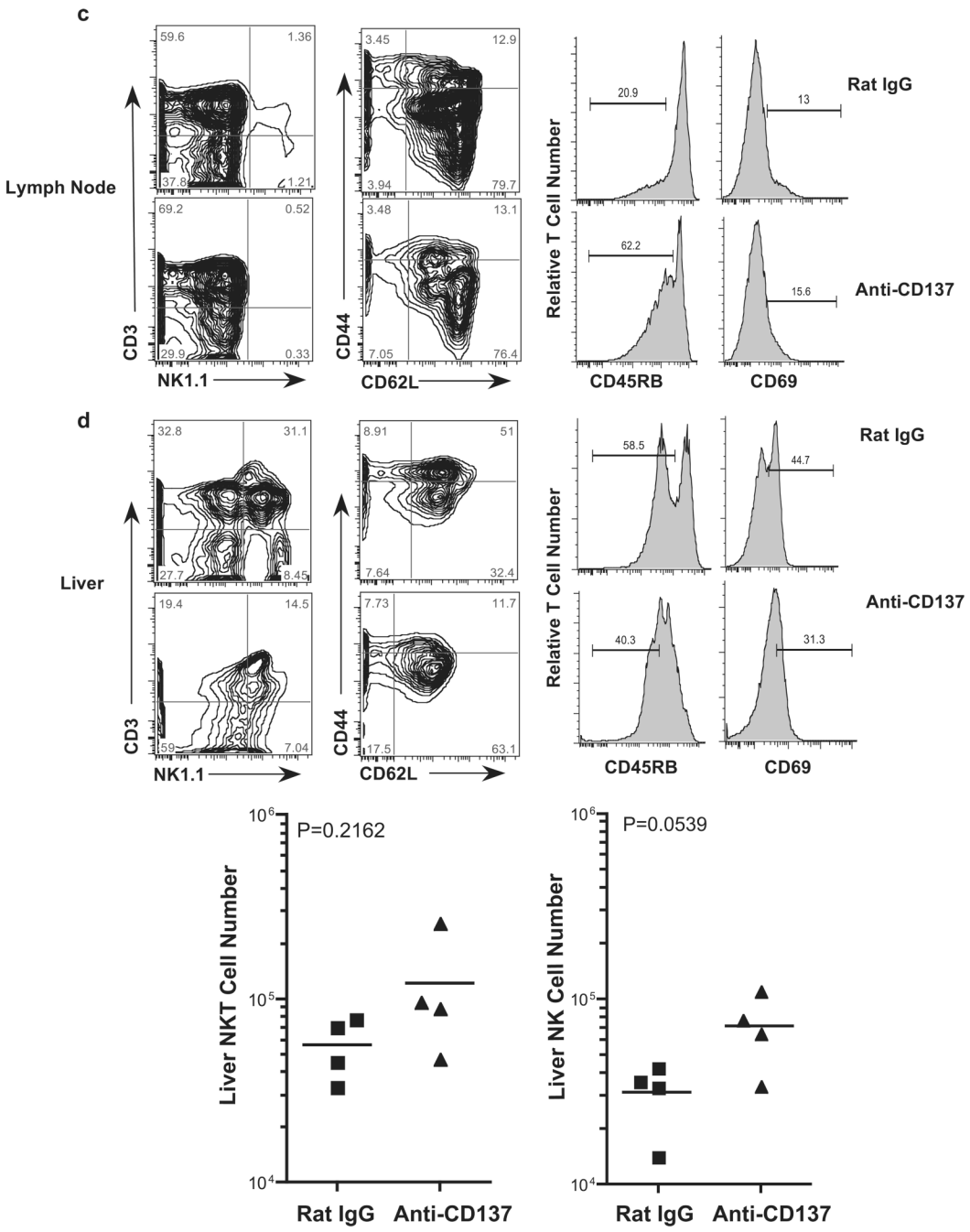

NIH-PA Author Manuscript

NIH-PA Author Manuscript

NIH-PA Author Manuscript

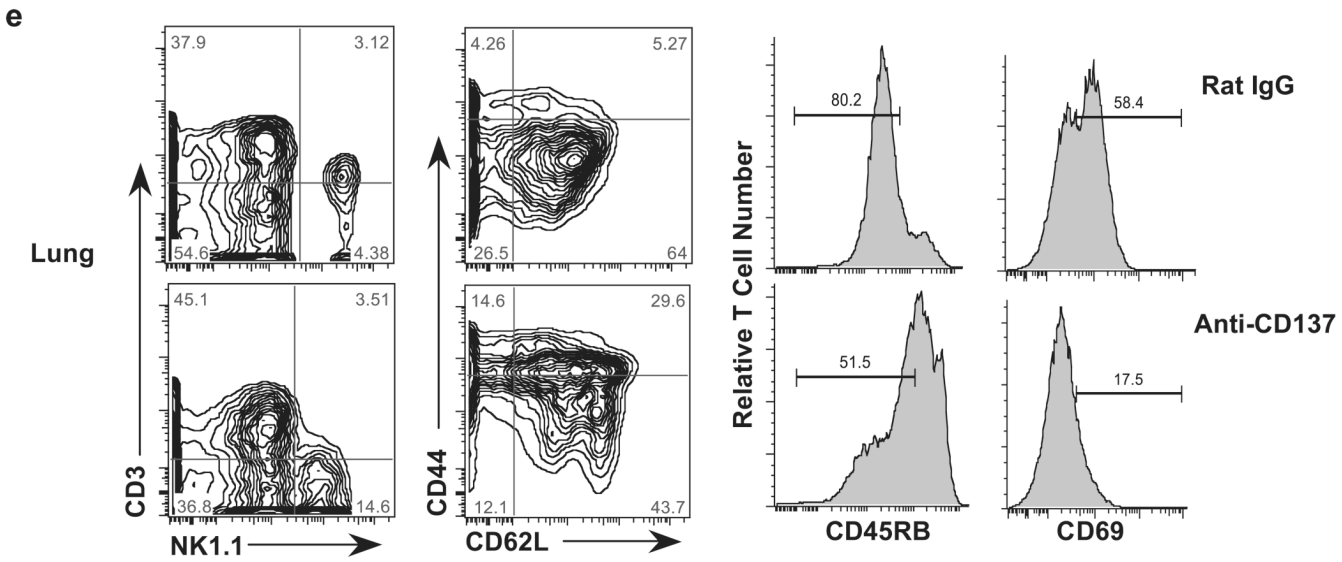

FIGURE 2.

Spleen and LN cell numbers. *a*, Total spleen cell numbers (rectangle represents mice within spleen cells within the normal range) as well as T and B cell numbers from spleens and inguinal LNs obtained from anti-CD137- or rat IgG-injected mice for the indicated periods were determined following FACS analysis. CD137- or rat IgG-injected mice were collected 1 wk after the indicated number of injections. Cell numbers in lymphoid tissues of rat IgG-injected mice varied by <10% over the course of three weekly injections, and the time point shown in all figures is of mice that received three injections. *b–e*, Single-cell suspensions of spleen, LN, liver, and lung, respectively, from anti-CD137- or rat IgG-injected mice were phenotyped 1 wk following three weekly injections for T, NK, and NKT cells; CD44, CD62L, CD45RB, and CD69 expression was measured on T cells.

NIH-PA Author Manuscript

NIH-PA Author Manuscript

NIH-PA Author Manuscript

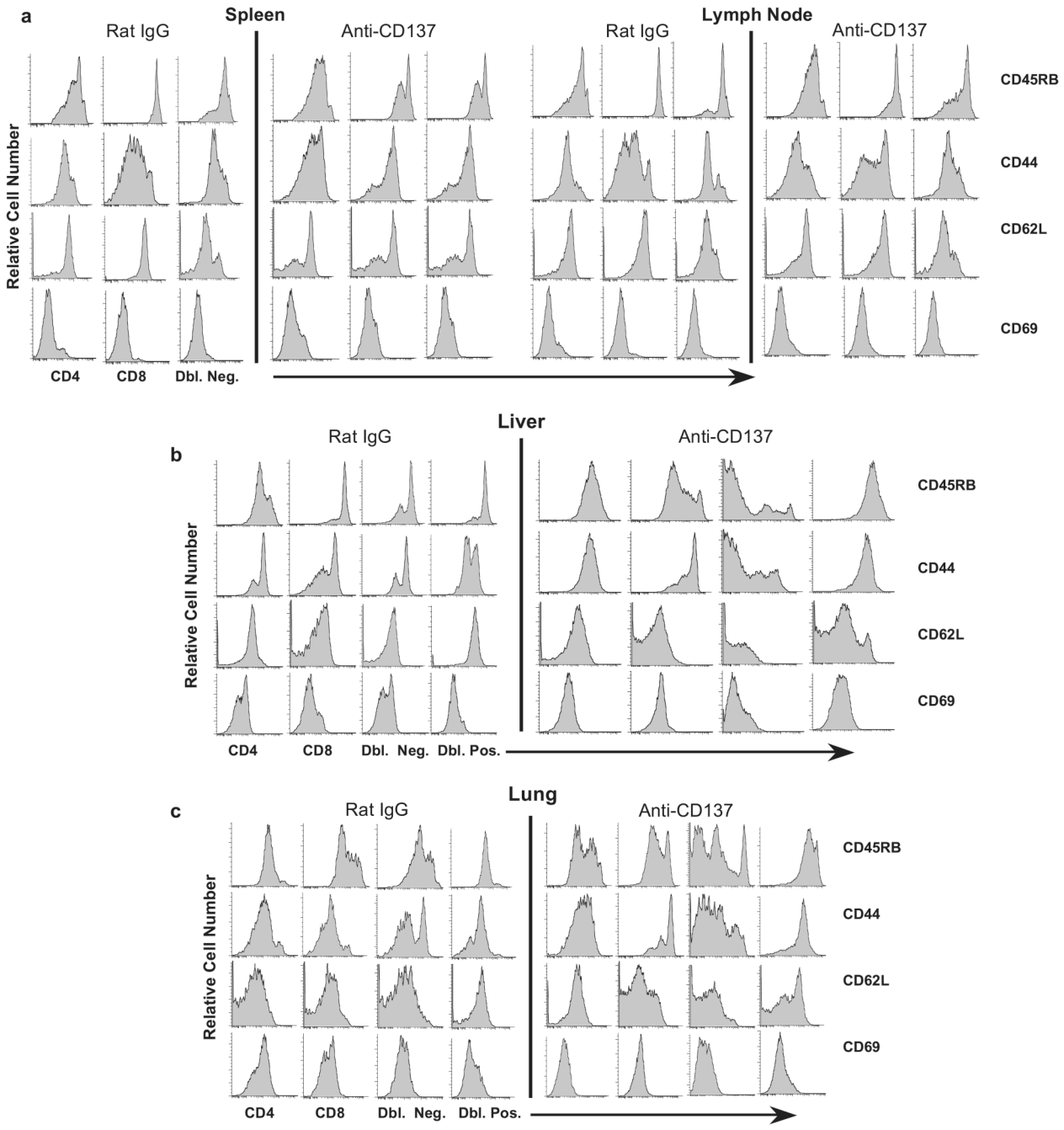

FIGURE 3.

Phenotypic analysis of T cell subsets. $CD3^+CD4^+$, $CD3^+CD8^+$, $CD3^+CD4^+CD8^+$, and $CD3^+CD4^-CD8^-$ T cell subsets from the spleen (*a*), LNs (*a*), livers (*b*), and lungs (*c*) of anti-CD137- or rat IgG-injected mice (weekly × 3) were phenotyped 1 wk following the final injection of Ab. The data are representative of one of five mice/group, and the experiment was repeated twice.

NIH-PA Author Manuscript
NIH-PA Author Manuscript
NIH-PA Author Manuscript

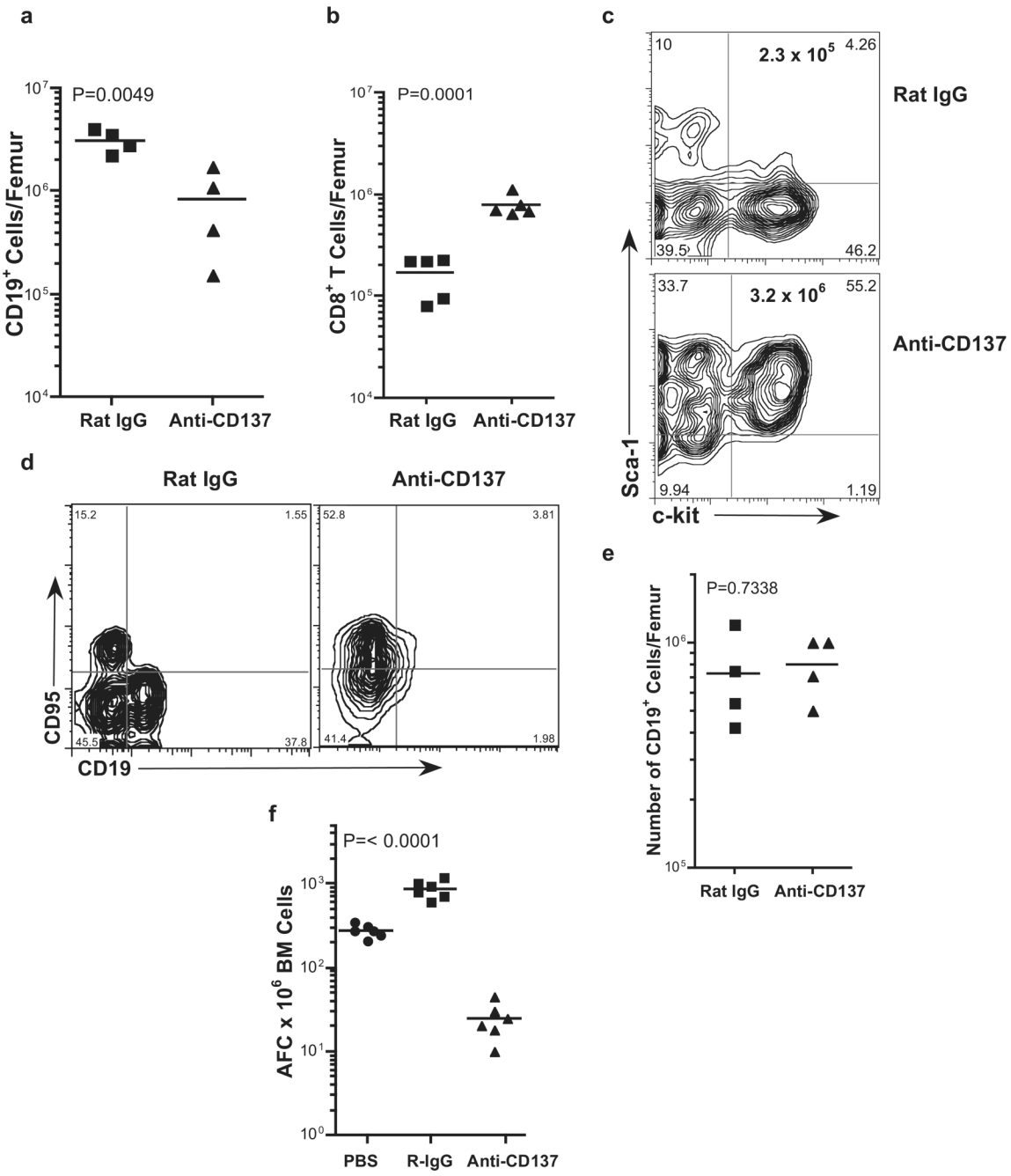

FIGURE 4.

B cells, BM, and ASC. BM cells were obtained from the femurs of rat IgG- and anti-CD137-treated mice that had received weekly injections of 200 μg of Ab over a 5-wk period. The mice were euthanized 1 wk later, and single-cell suspensions were prepared by passage through 70-mesh nylon screens, counted for cell viability, stained with the indicated fluorochrome-conjugated mAbs, and analyzed by flow cytometry. The absolute number of *a*, $CD19^+$ cells; *b*, $CD8^+$ cells; *c*, c-*kit*$^+$ Sca-1^+ Lin^- hemopoietic stem cells (KSL); and *d*, Fas^+ cells was determined by FACS analysis. *e*, The number of $CD19^+$ BM cells/femur was determined in C57BL/6 IFN-γ-deficient mice injected with either rat IgG or anti-CD137, as described

above.*f*, The number of IgG-secreting BM cells/femur of Ab-treated mice was determined by ELISPOT assay.

NIH-PA Author Manuscript
NIH-PA Author Manuscript
NIH-PA Author Manuscript

NIH-PA Author Manuscript
NIH-PA Author Manuscript
NIH-PA Author Manuscript

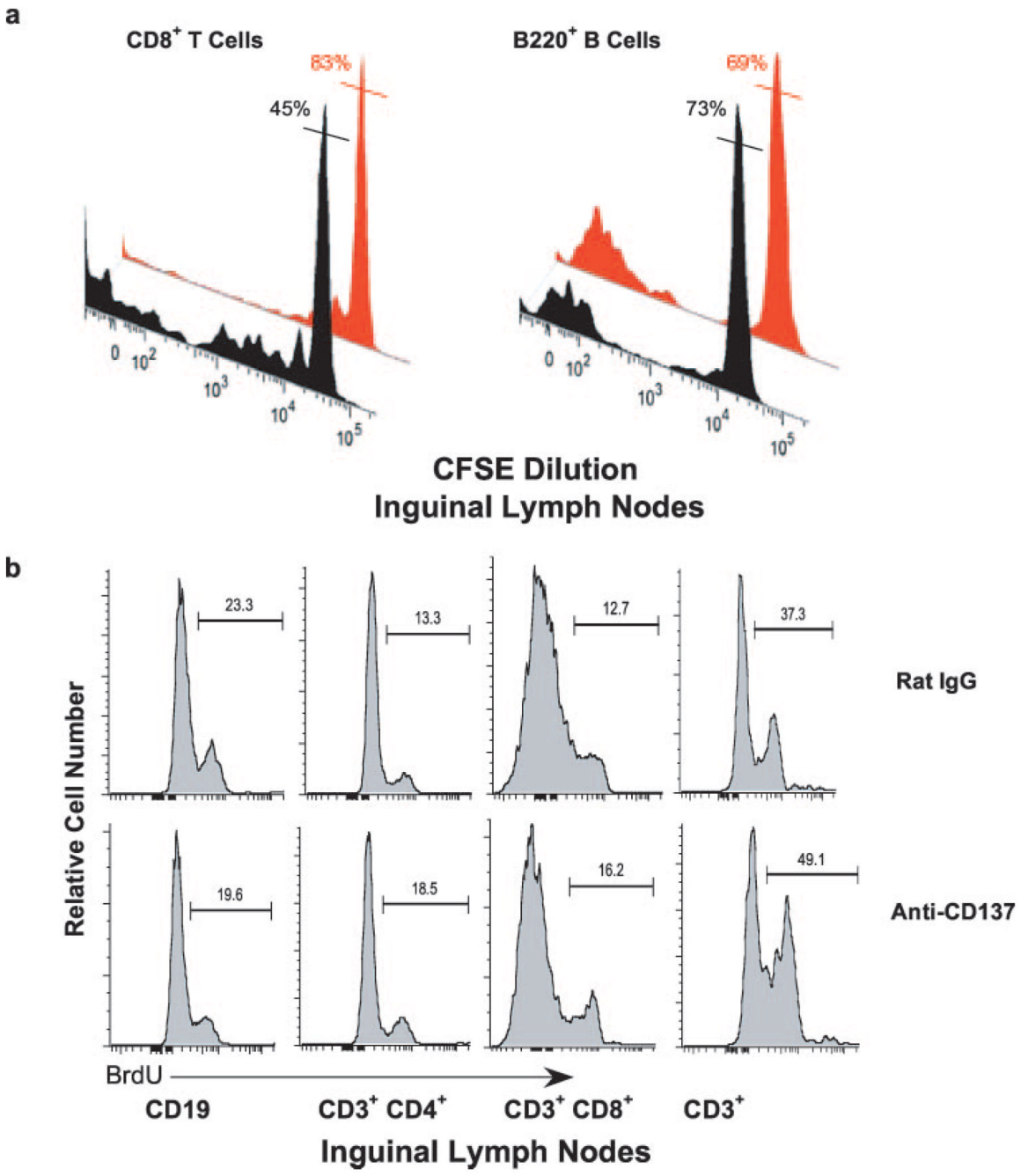

FIGURE 5.

a, In vivo proliferation of LN CD8 T cells and B220 B cells was conducted by adoptively transferring CFSE-labeled BL/6 CD45.1 congenic spleen cells into wild-type CD45.2 BL/6 mice before treating the mice with five weekly injections of 200 μg of anti-CD137 or rat IgG. FACS analysis was performed at week 6. CD45.1 $CD3^+CD8^+$ T cell and $CD19^+$ B cell proliferation was determined by CFSE dilution. Black histograms represent CD137-treated mice, and red histograms represent rat IgG-treated mice. The percentages shown for each histogram represent the frequency of nondividing cells in each gated population denoted by the horizontal bar intersecting the histogram peak. *b*, Inguinal LN B and T cell proliferation

was also determined by BrdU short pulse labeling for 4 h following the third weekly injection of anti-CD137 or rat IgG.

NIH-PA Author Manuscript
NIH-PA Author Manuscript
NIH-PA Author Manuscript

NIH-PA Author Manuscript

NIH-PA Author Manuscript

NIH-PA Author Manuscript

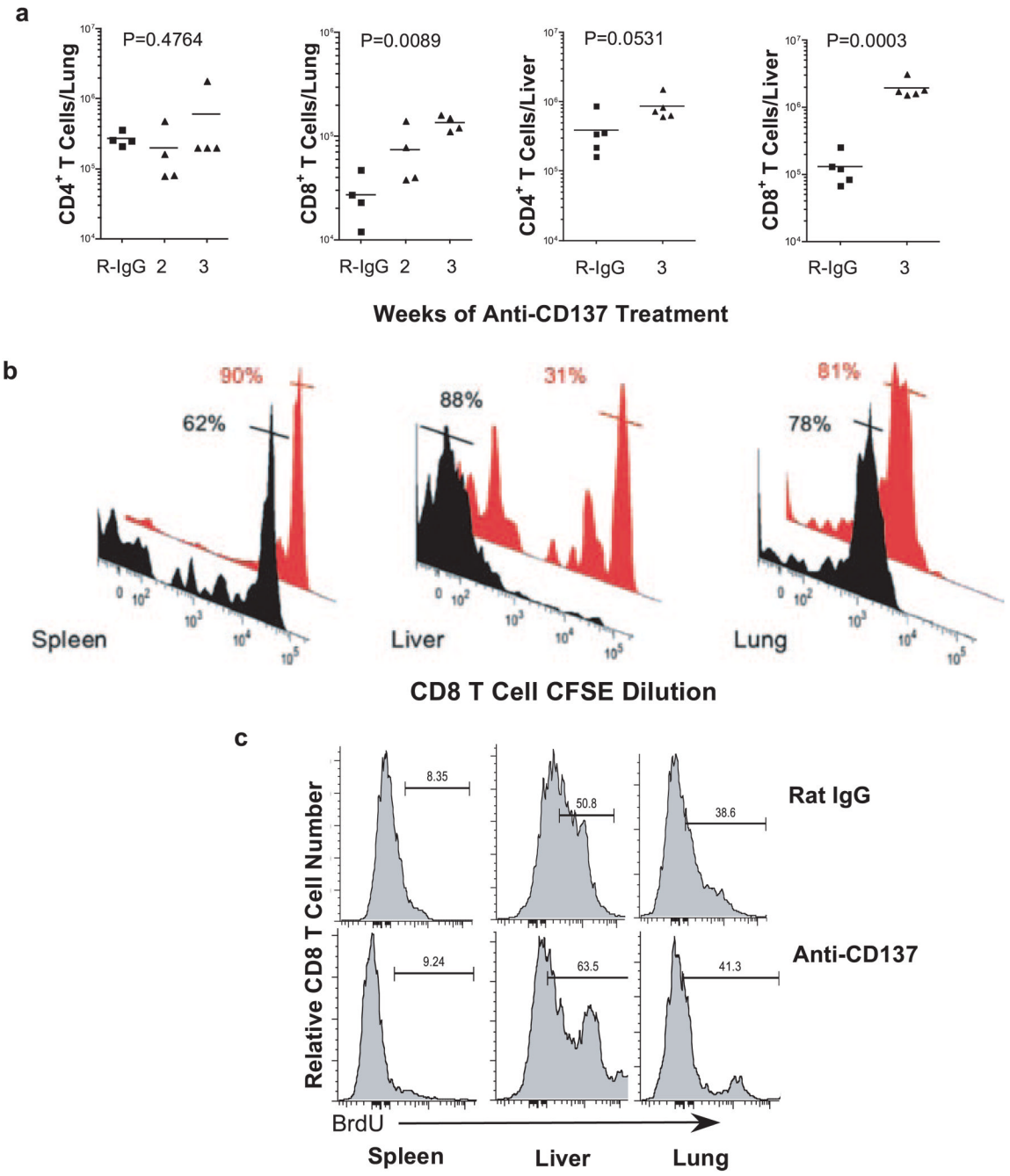

FIGURE 6.

Liver- and lung-infiltrating T cells, and CD8 T cell proliferation. *a*, Absolute numbers of lung and liver CD4 and CD8 T cells from rat IgG- and anti-CD137 mAb-treated mice were determined by FACS analysis 1 wk after the fifth weekly injection of Ab. *b*, CD8 T cell proliferation was determined by gating on CFSE-labeled CD45.1 BL/6 CD8 T cells in the spleen, liver, and lungs of anti-CD137 (black histograms)- or rat IgG (red histograms)-injected mice. Percentages represent the frequency of cells in the gated regions indicated by horizontal bars intersecting the peaks. *c*, Proliferation was also determined by BrdU short pulse labeling for 4 h following the final weekly injection of anti-CD137 or rat IgG.

NIH-PA Author Manuscript
NIH-PA Author Manuscript
NIH-PA Author Manuscript

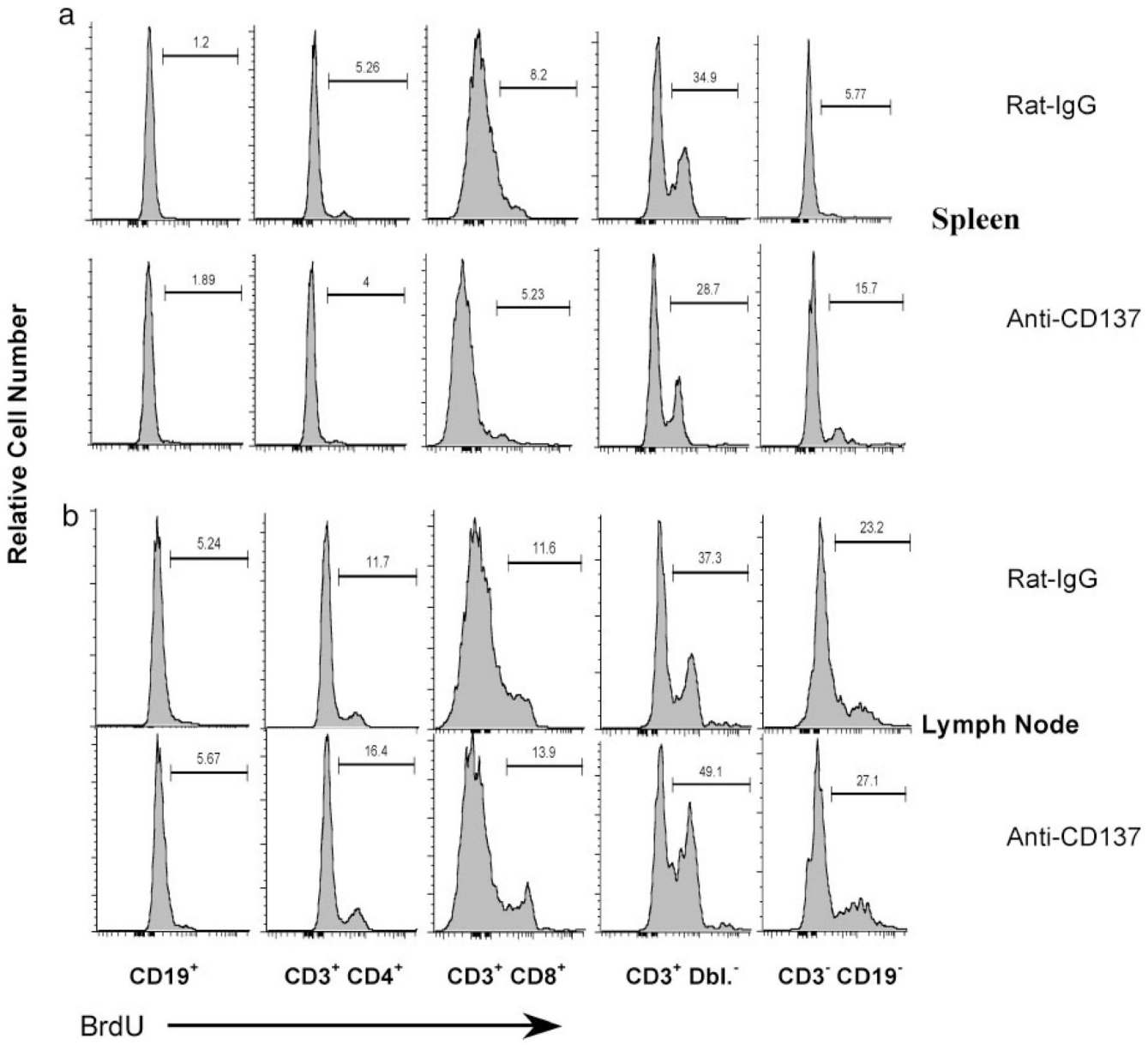

NIH-PA Author Manuscript
NIH-PA Author Manuscript
NIH-PA Author Manuscript

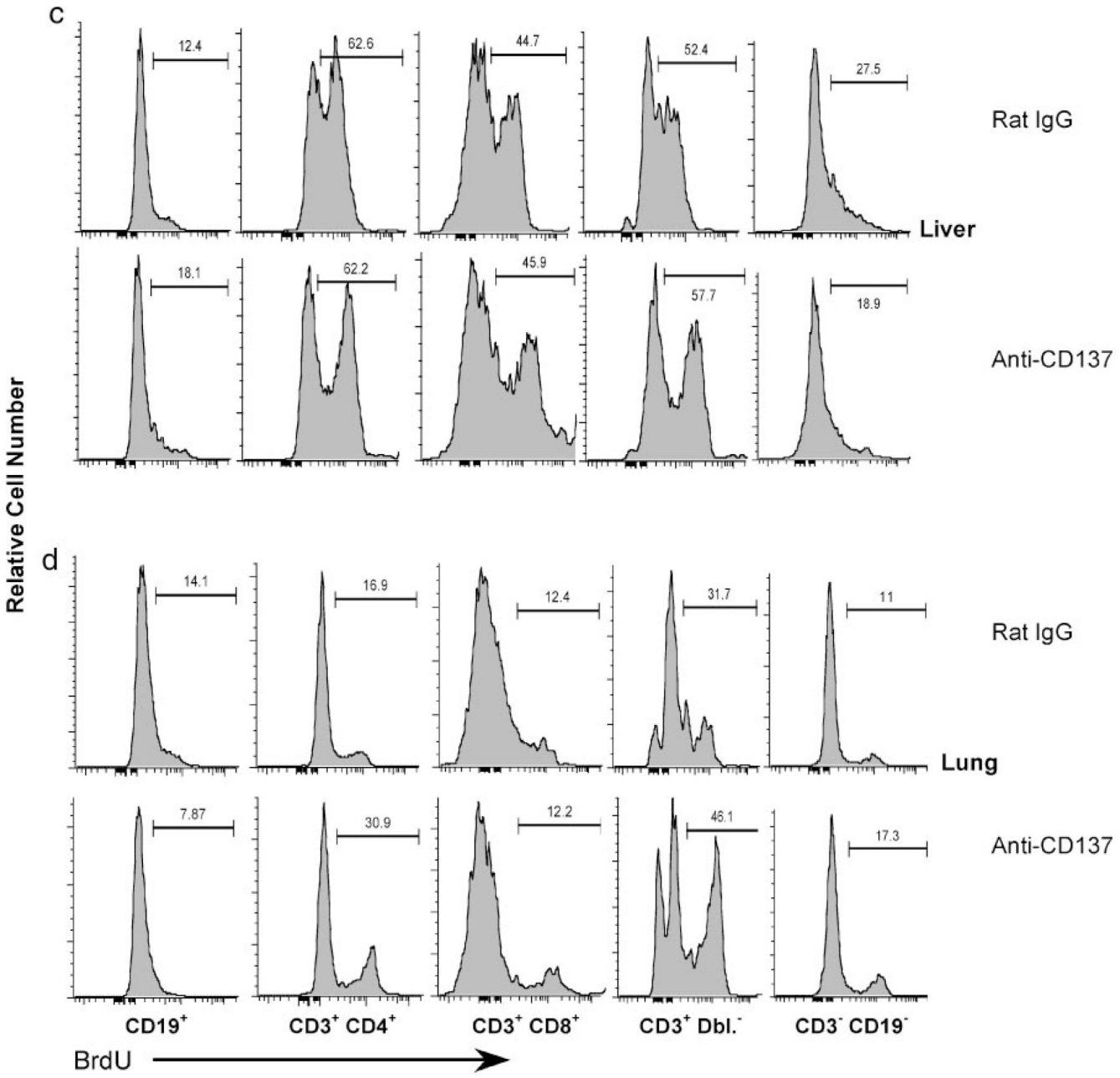

FIGURE 7.

Lymphocyte proliferation. Lymphocyte proliferation in the spleen (*a*), LN (*b*), liver (*c*), and lung (*d*) was assessed following a 4-h pulse with BrdU (2 mg in 0.2 ml of PBS) injected i.p. 24 h following the third weekly injection of 200 μg of either rat IgG or anti-CD137 mAb. All animals were euthanized, and single-cell suspensions were prepared and surface stained with the indicated fluorochrome-conjugated mAbs. The cells were then permeabilized and stained with FITC anti-BrdU following the manufacturer's protocol (BD Immunocytometry Systems) and analyzed by multicolor flow cytometry using a LSR II multiparameter flow cytometer (BD Immunocytometry Systems). No differences were observed between controls and treated groups in the thymus and BM (data not shown).

NIH-PA Author Manuscript
NIH-PA Author Manuscript
NIH-PA Author Manuscript

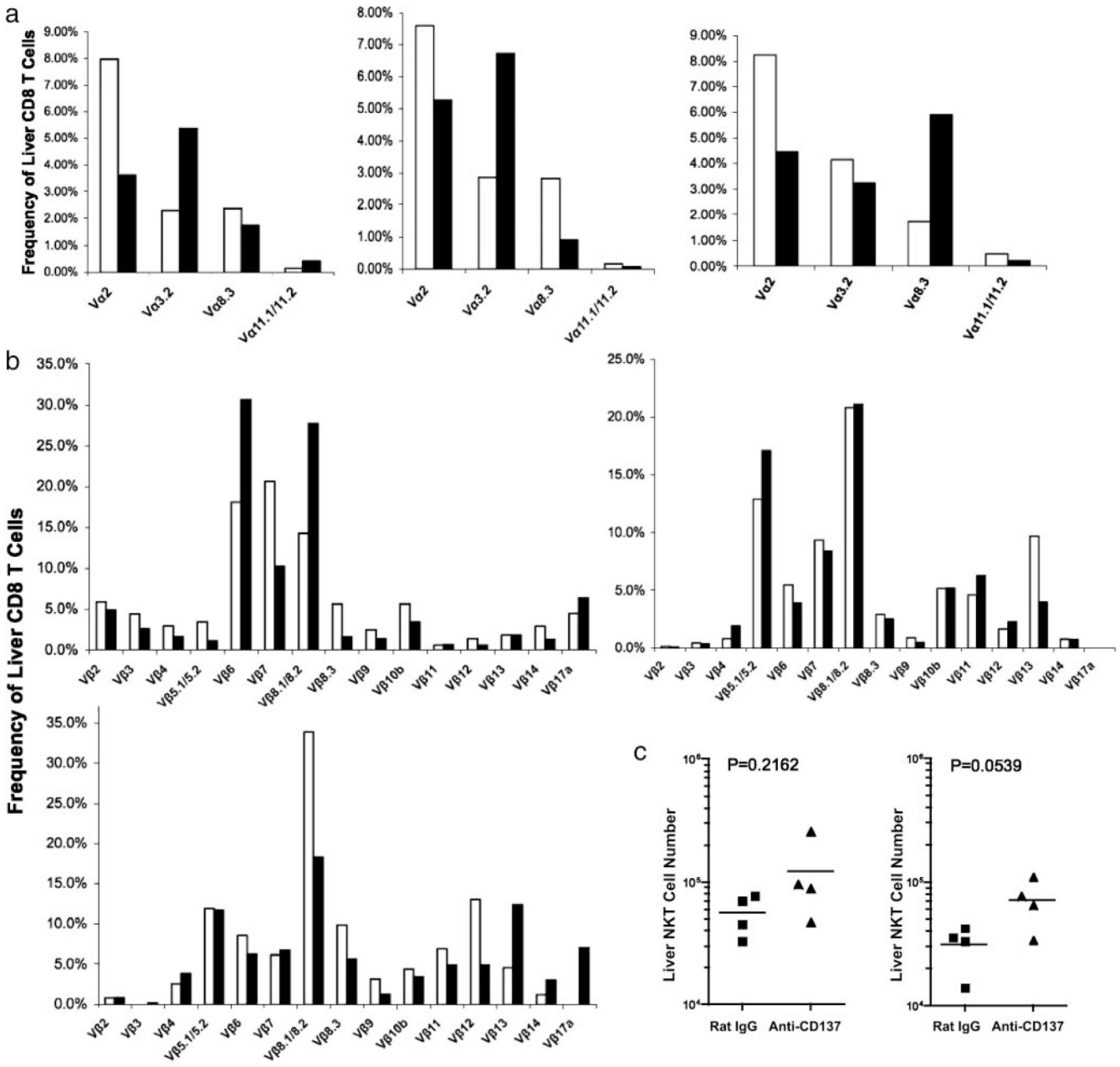

FIGURE 8.

TCR Vαβ usage by liver-infiltrating CD8 T cells and liver NK/NKT cells. *a* and *b*, TCR Vα and Vβ usage, respectively, by liver-infiltrating CD8 was determined in three separate experiments by staining CD8 T cells with fluorochrome-conjugated mAbs specific for individual Vαβ gene products, followed by FACS analysis 1 wk following the last of three weekly 200-μg injections of anti-CD137 or rat IgG. *c*, The absolute number of liver-infiltrating NK and NKT T cells was determined by flow cytometry following staining with anti-CD3 and NK1.1.

NIH-PA Author Manuscript
NIH-PA Author Manuscript
NIH-PA Author Manuscript

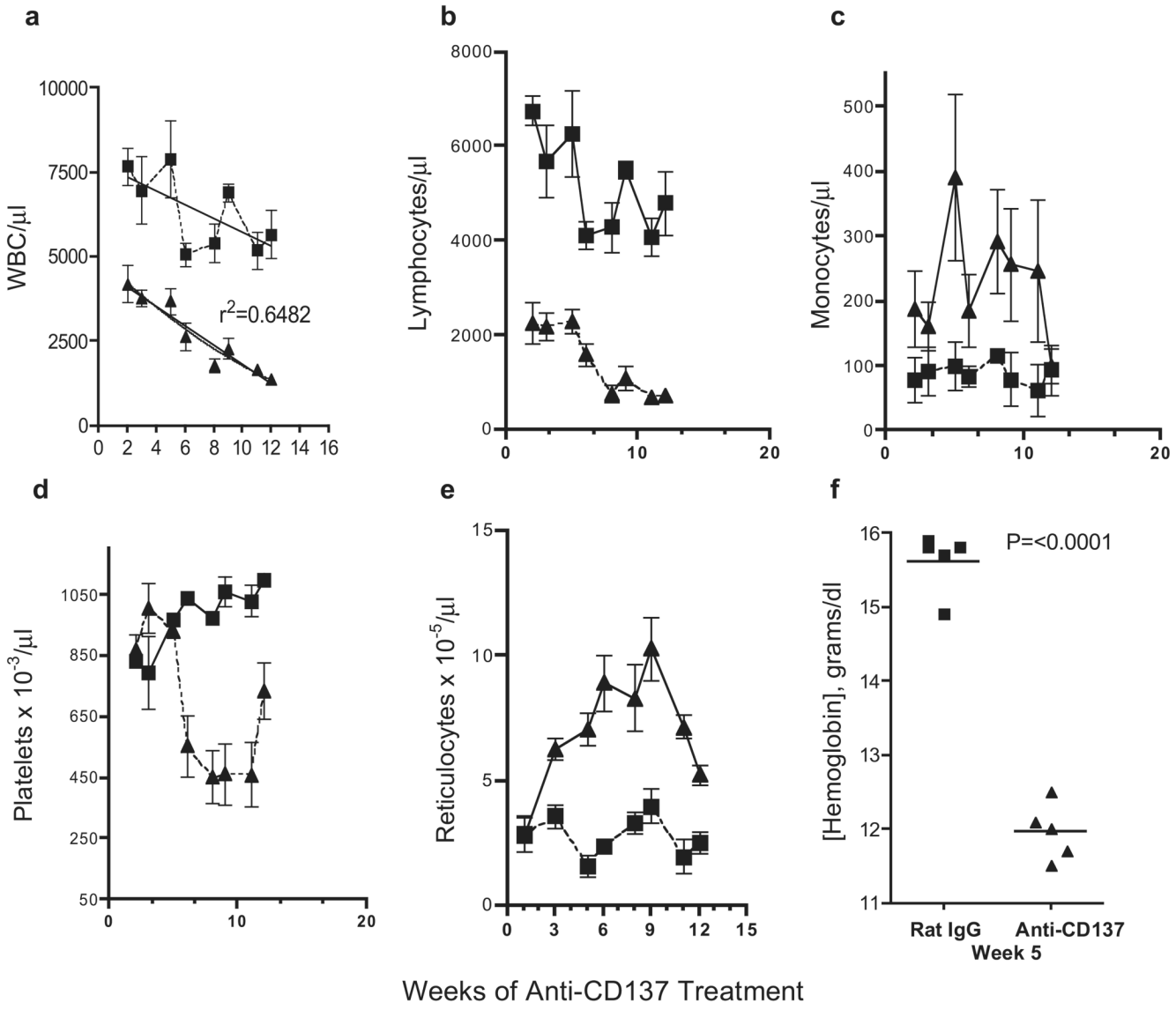

FIGURE 9.

Peripheral mononuclear cells and blood elements. CBC were determined in anti-CD137 (▲)- and rat IgG (■)-treated mice ($n = 5$) and analyzed. *a*, White blood cells/µl whole blood. *b*, Total number of lymphocytes/µl whole blood. *c*, Total number of monocytes/µl whole blood. *d*, Total number of platelets × 10^{-3}/µl whole blood. *e*, Total number of reticulocytes × 10^{-5}/µl whole blood.*f*, Hemoglobin concentration.

NIH-PA Author Manuscript
NIH-PA Author Manuscript
NIH-PA Author Manuscript

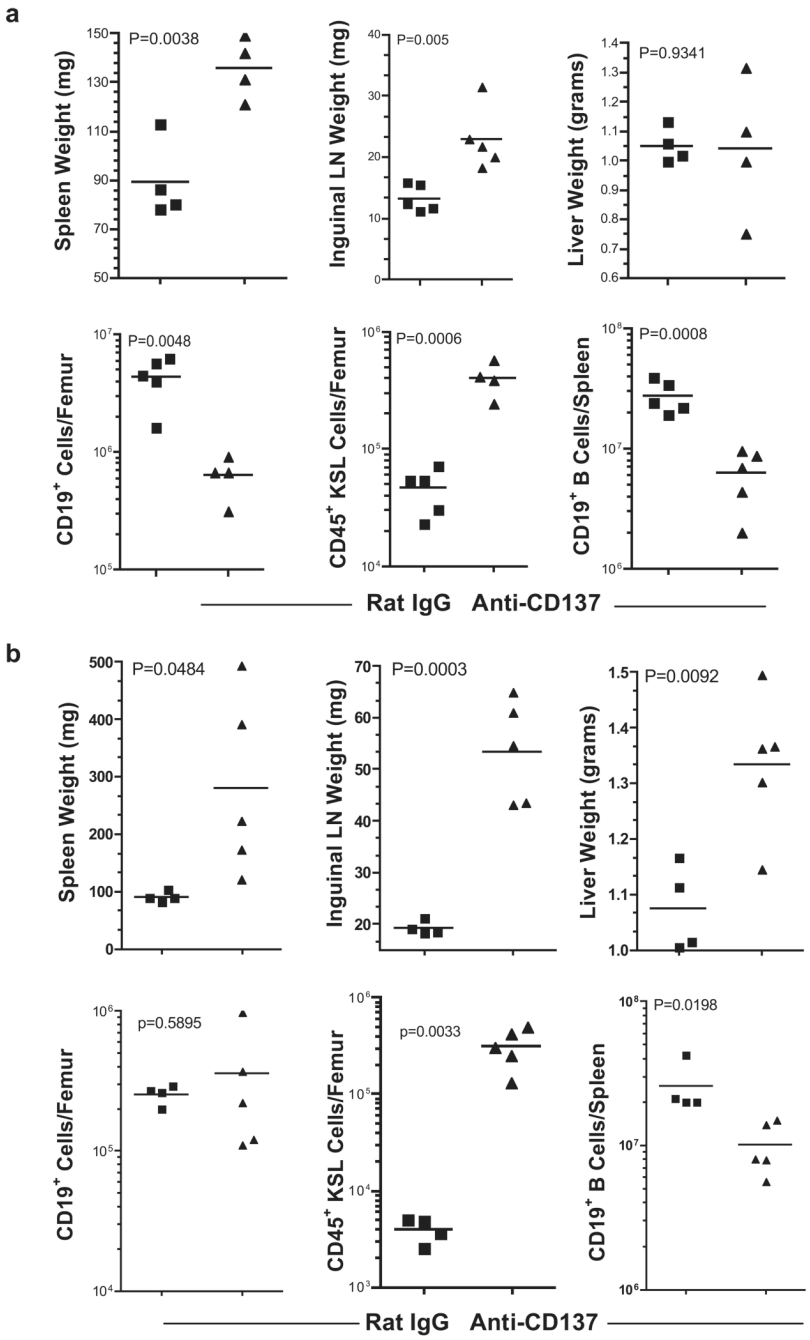

FIGURE 10.

Anti-CD137 treatment of CD8- or CD4-deficient mice. *a* and *b*, Spleens, inguinal LNs, and livers from C57BL/6 CD8-or CD4-deficient mice, respectively, were collected 1 wk following the fifth weekly injection of anti-CD137 or rat IgG mAb and weighed. BM from the femurs was prepared and pheno-typed by FACS, and the number of BM $CD19^+$ and KSL (c-kit^+ $Sca\text{-}1^+$ Lin^-) cells was determined.

NIH-PA Author Manuscript

NIH-PA Author Manuscript

NIH-PA Author Manuscript

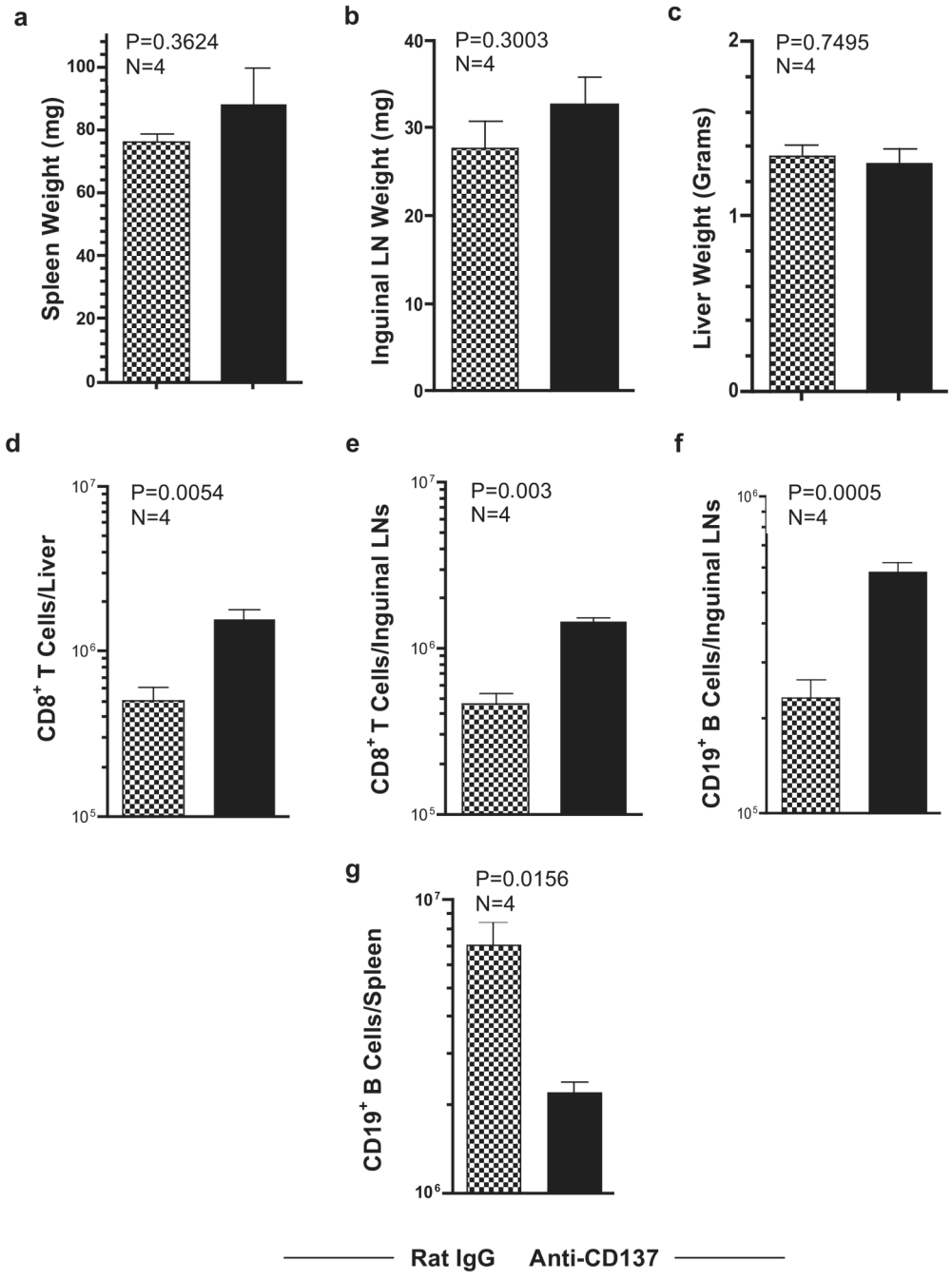

FIGURE 11.

Anti-CD137 treatment of TNF-α-deficient mice. BL/6 TNF-$\alpha^{-/-}$ mice were injected i.p. with 200 μg of rat IgG or anti-CD137 mAbs 1 × weekly for 3 wk. The following week, the mice were bled and euthanized. Spleen, inguinal LNs, and livers were weighed (*a–c*), and tissues were processed into single-cell suspensions, stained for CD8 T and CD19-positive B cells, and analyzed by FACS. From FACS frequency plots and microscopic count of viable cells, absolute numbers of liver and LN CD8 T cells were determined (*d* and *e*, respectively), and LN and splenic CD19 B cells were determined (*f* and *g*, respectively).

NIH-PA Author Manuscript

NIH-PA Author Manuscript

NIH-PA Author Manuscript

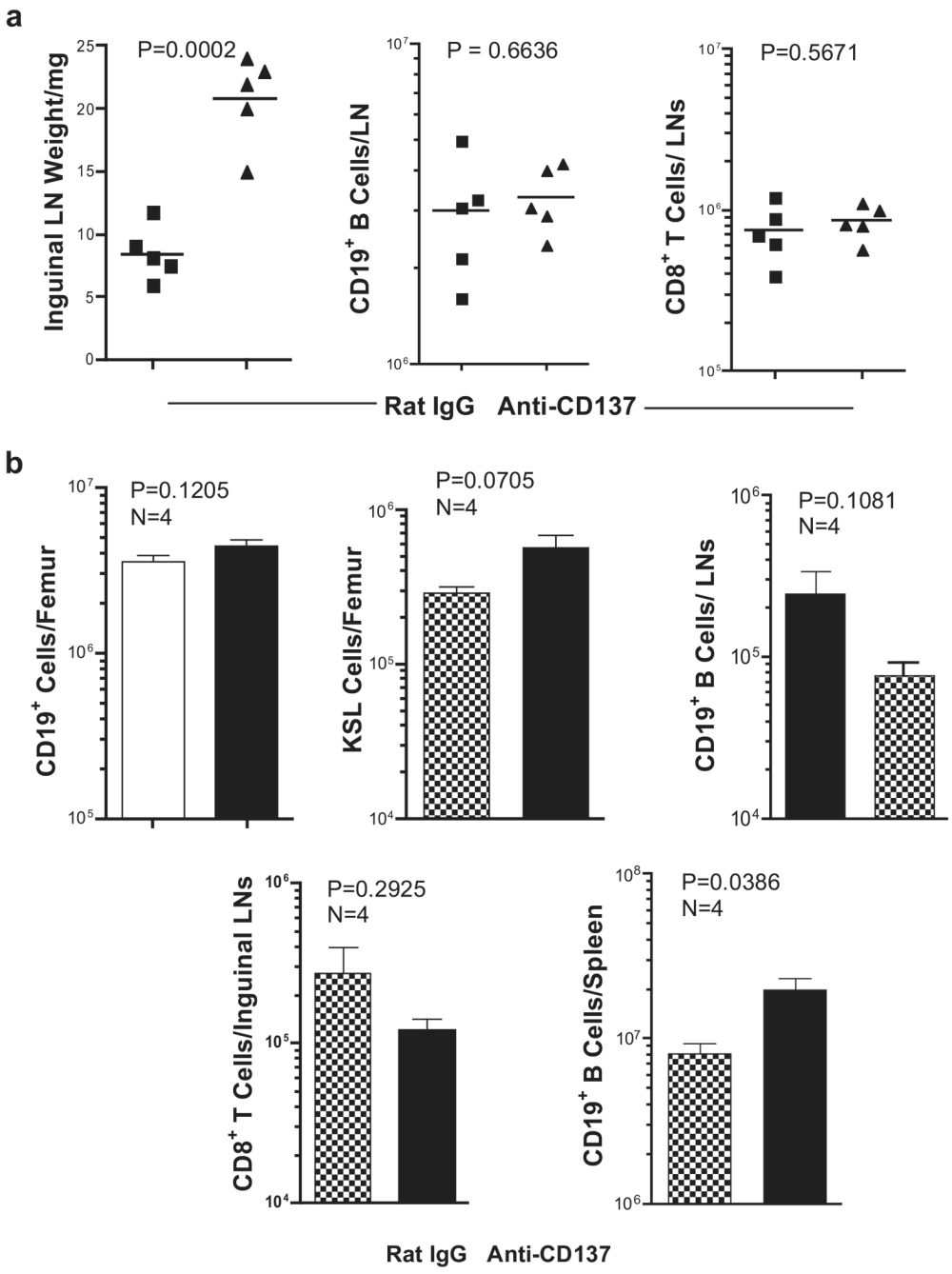

FIGURE 12.

Anti-CD137 treatment of IFN-γ- and IFN-αR-deficient mice. *a*, Inguinal LNs from IFN-γ-deficient mice were collected 1 wk following the third weekly injection of anti-CD137 or rat IgG, weighed and processed into single-cell suspensions, and phenotyped by FACS to determine total B cell and CD8 T cell numbers. *b*, BM, inguinal LNs, and spleens were collected from IFN-αR-deficient mice, as above. $CD19^+$ cell, KSL cell, and $CD8^+$ T cell numbers were determined in single-cell suspensions stained with fluorochrome-conjugated anti-CD19, anti-CD3, anti-CD8, anti-c-*kit*, anti-Sca-1, and lineage-specific mAbs. B cells, KSL cells, and CD8 T cells were enumerated following FACS analysis.